

MapReduce LoRA: Advancing the Pareto Front in Multi-Preference Optimization for Generative Models

Chieh-Yun Chen¹, Zhonghao Wang^{2†}, Qi Chen², Zhifan Ye¹, Min Shi¹, Yue Zhao¹,
Yinan Zhao², Hui Qu², Wei-An Lin², Yiru Shen², Ajinkya Kale², Irfan Essa¹, Humphrey Shi^{1†}

¹Georgia Tech ²Adobe

github.com/SHI-Labs/MapReduce-LoRA

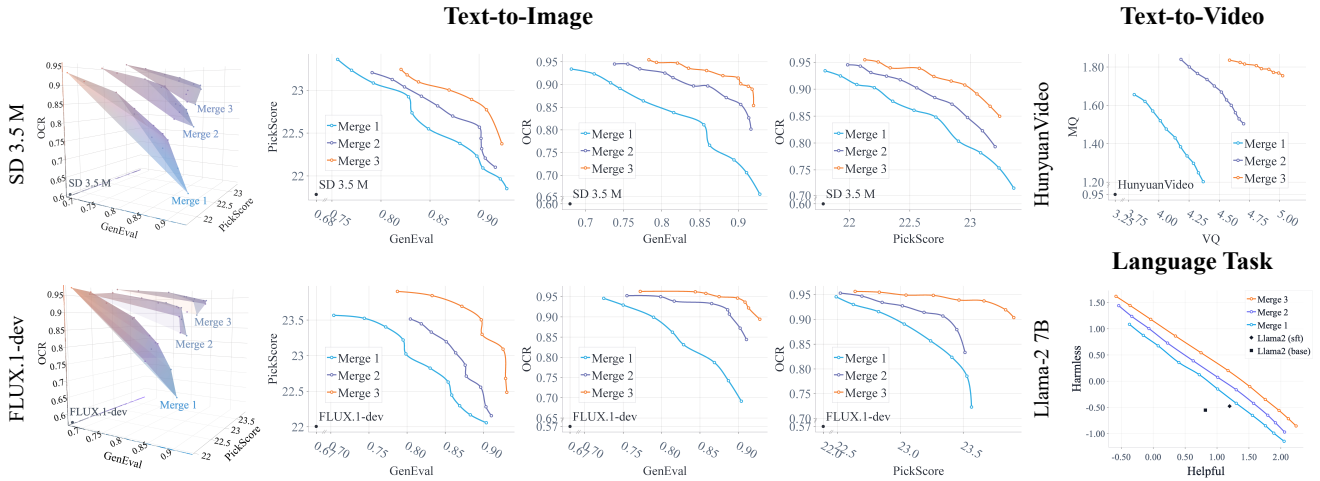


Figure 1. **MapReduce LoRA advances the Pareto fronts on Text-to-Image, Text-to-Video and language tasks.** Left: On Stable Diffusion 3.5 Medium [2] (top) and FLUX.1-dev [20] (bottom), we plot the 3D Pareto front over GenEval [14], PickScore [18], and OCR [8] (Column 1), and the 2D Pareto fronts where one reward weight is set to zero (Columns 2–4). Right (top): On HunyuanVideo [19], we plot the 2D Pareto front over Visual Quality (VQ) and Motion Quality (MQ). Right (bottom): On Llama-2 7B [42] (following Bone Soup [44]’s setup), we plot the 2D Pareto front on Helpful Assistant task over helpful and harmless rewards. *Please refer to the Supplement D.1 and A for full results.*

Abstract

Reinforcement learning from human feedback (RLHF) with reward models has advanced alignment of generative models to human aesthetic and perceptual preferences. However, jointly optimizing multiple rewards often incurs an alignment tax—improving one dimension while degrading others. To address this, we introduce two complementary methods: MapReduce LoRA and Reward-aware Token Embedding (RaTE). MapReduce LoRA trains preference-specific LoRA experts in parallel and iteratively merges them to refine a shared base model; RaTE learns reward-specific token embeddings that compose at inference for flexible preference control. Experiments on Text-to-Image generation (Stable Diffusion 3.5 Medium and FLUX.1-dev) show improvements of 36.1%, 4.6%, and 55.7%, and

32.7%, 4.3%, and 67.1% on GenEval, PickScore, and OCR, respectively. On Text-to-Video generation (HunyuanVideo), visual and motion quality improve by 48.1% and 90.0%, respectively. On the language task, Helpful Assistant, with Llama-2 7B, helpful and harmless improve by 43.4% and 136.7%, respectively. Our framework sets a new state-of-the-art multi-preference alignment recipe across modalities.

1. Introduction

Recent progress in Text-to-Image [2, 9, 11, 20] and Text-to-Video [19, 34, 43] has been driven by flow-based diffusion models [25, 28], achieving unprecedented visual fidelity. To better align outputs with human judgment, post-training methods, particularly reinforcement learning from human feedback (RLHF) [26, 35, 38, 45], have become es-

[†]Corresponding authors.

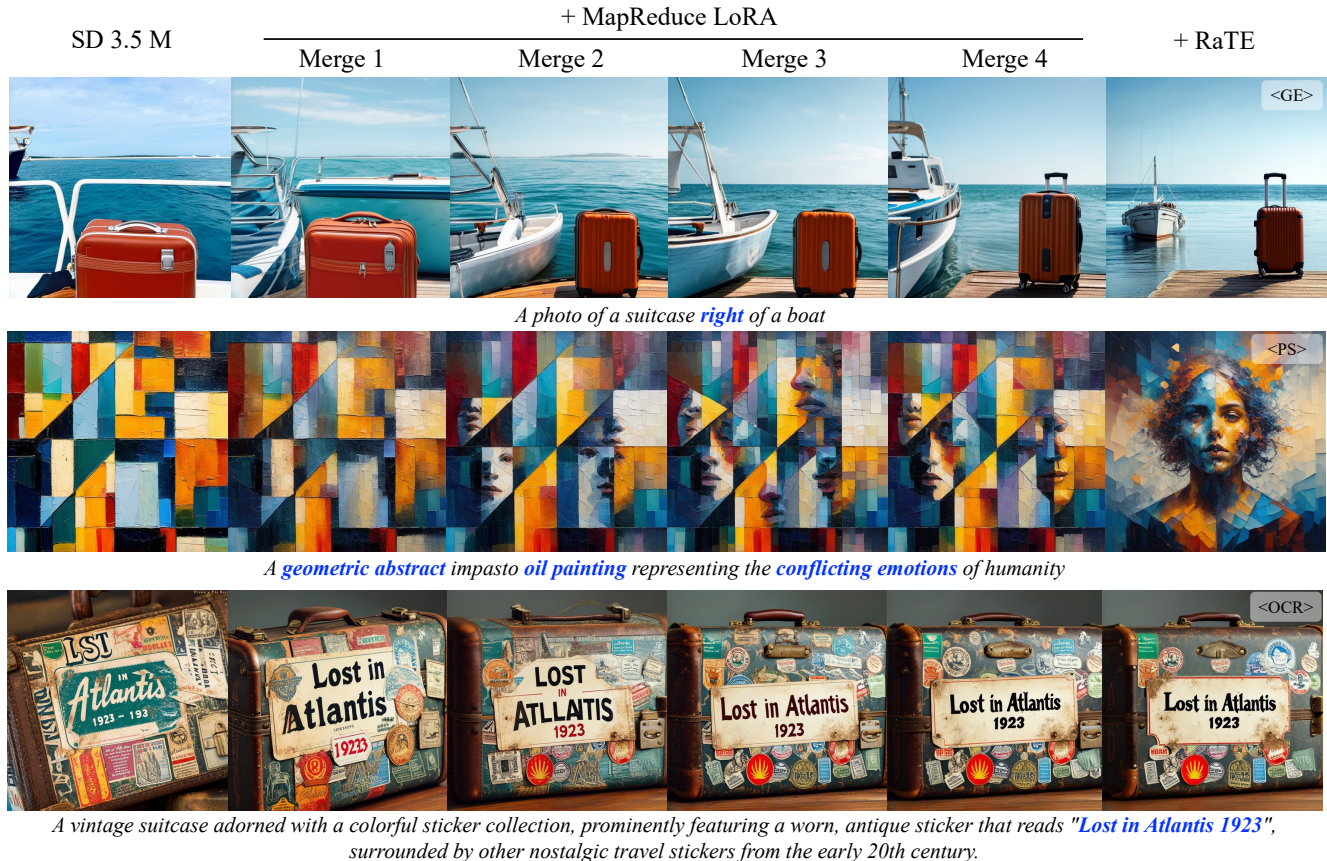


Figure 2. **MapReduce LoRA** progressively advances performance across iterations; **Reward-aware Token Embedding (RaTE)** enables flexible preference control.

sential. Reward-based RLHF trains reward models from human annotations to capture specific evaluation criteria, and optimizes the generator by sampling generations, scoring them with the reward models, and updating parameters with reward-weighted objectives. However, human perception of quality is inherently multi-dimensional. In practice, multiple reward models are used to reflect criteria such as text-image alignment [14, 24], aesthetic quality [17], text rendering [8], and overall preference [18, 30]. This raises a central challenge: how to optimize generative models that can improve across multiple preferences simultaneously without sacrificing any single dimension.

While post-training methods [26, 45] perform well under a single reward, they either degrade on unoptimized metrics at evaluation time or suffer competing gradients when jointly optimizing multiple rewards—two manifestations of the alignment tax. Multi-objective reinforcement learning (MORL) [1, 21, 23, 36] attempts to optimize multiple rewards simultaneously by combining rewards through weighted mixtures or approximating a Pareto set with test-time weight control. However, weighted mixtures are dominated by easily optimized objectives, leaving harder preferences under-trained or even regressed. Calibrated Prefer-

ence Optimization (CaPO) [21] partially addresses this imbalance but remains limited by fixed weighting and modest performance gains. Rewarded Soup [36] offers a posteriori weight selection but still lags behind models fine-tuned individually per reward. Consequently, existing approaches struggle to deliver models that generalize well across diverse reward signals. Achieving a unified framework that improves multiple human-aligned preferences efficiently and robustly remains a fundamental challenge in multi-objective post-training.

To address these limitations, we propose two complementary approaches—MapReduce LoRA and Reward-aware Token Embedding (RaTE)—that jointly advance multi-preference alignment. MapReduce LoRA decomposes multi-objective optimization into i) a Map phase that trains reward-specific LoRA experts in parallel, and ii) a Reduce phase that merges experts with user-controlled interpolation, folds the merged adapter into the base, and iterates to advance the Pareto front. Complementarily, RaTE introduces a lightweight inference-time control by assigning each reward a learned token embedding, enabling composable conditioning by appending multiple tokens to the input prompt. Together, MapReduce LoRA and RaTE en-

able a posteriori customization without retraining, yielding unified generative models that excel across multiple reward dimensions.

Extensive experiments demonstrate that our proposed methods substantially advance the Pareto front of multi-preference alignment across both Text-to-Image, Text-to-Video generation, and Language Tasks (Fig. 1). On Stable Diffusion 3.5 Medium [2] and FLUX.1-dev [20], our method improves GenEval [14], PickScore [18], and OCR [8] by 36.1%, 4.6%, 55.7% and 32.7%, 4.3%, 67.1%, respectively. Beyond in-domain metrics, untargeted rewards—*i.e.*, VQAScore [24], MPS [47], and VILA [17]—also improve by 1.85%, 6.49%, and 19.96%, validating the robustness and scalability of our method. On HunyuanVideo [19], visual and motion quality improve by 48.1% and 90.0%, achieving state-of-the-art results among post-trained diffusion systems. On Llama-2 7B [42], helpful and harmless improve by 43.4% and 136.7%, respectively. Collectively, these results highlight the effectiveness of combining MapReduce LoRA and RaTE for efficient, controllable, and human-aligned generation. Our contributions are fourfold:

- We introduce MapReduce LoRA, a scalable multi-reward training framework that iteratively advances the Pareto front across preferences.
- We propose Reward-aware Token Embedding for flexible, composable inference-time control of reward trade-offs.
- MapReduce LoRA achieves state-of-the-art performance on Text-to-Image, Text-to-Video and language tasks, with substantial multi-rewards gains.
- MapReduce LoRA exhibits strong generalization to untargeted rewards, demonstrating robust cross-preference alignment.

2. Related Work

2.1. Flow-based Generative Models

Flow Matching (FM) [25] trains continuous normalizing flows by regressing the conditional velocity field along a path between the data distribution and a standard normal, yielding a score-free, simulation-free objective with more stable and efficient optimization than diffusion losses. Rectified Flow (RF) [28] specializes FM to a straight-line, approximately constant-speed path, rectifying trajectories and simplifying supervision, which improves stability and sampling efficiency. Recent Text-to-Image [2, 6, 9, 11, 20] and Text-to-Video [19, 34, 43] methods adopt FM/RF to learn the velocity field directly, improving efficiency over diffusion-style denoising and often yielding stronger gradients for conditional generation.

2.2. Reinforcement Learning from Human Feedback (RLHF)

RLHF [7, 16] was first used to train agents in simulators and Atari, and later to fine-tune language models for summarization [40]. InstructGPT [32] scaled RLHF to align broad language tasks with a three-stage pipeline: supervised fine-tuning (SFT), reward-model training, and policy optimization with Proximal Policy Optimization (PPO) [38]. Direct Preference Optimization (DPO) [35] removes the reward model and online RL, directly optimizing the policy from human preference pairs. Group Relative Policy Optimization (GRPO) [39] is a PPO-style preference method that drops the critique and uses relative scores across multiple samples per prompt, improving stability and sample efficiency. To apply RL to diffusion models, Denoising Diffusion Policy Optimization (DDPO) [4] formulates the denoising process as a Markov Decision Process (MDP). Building on this MDP formulation, Flow-GRPO [26] and DanceGRPO [45] extend GRPO [39] to flow-based generative models by using an ODE-to-SDE strategy to inject stochasticity and overcome the determinism of standard flow models.

However, single-reward RLHF optimizes one preference dimension in isolation, while generative quality spans multiple and often conflicting objectives. This creates a natural bridge to **Multi-Objective RL (MORL)**, where the objective is to balance conflicting rewards and approximate a Pareto-optimal solution—precisely the challenge in post-training generative models. MORL methods can be categorized into two classes: *a priori* [1, 21], which scalarizes objectives into a single signal (*e.g.*, weighted sums), and *a posteriori* [23, 36], which approximate a Pareto set and enable test-time control. CaPO [21] calibrates and balances multiple T2I preferences, and MOPO [1] frames alignment as constrained, KL-regularized optimization; both are *a priori* and lack test-time control. Rewarded Soups [36] extends Linear Mode Connectivity [12, 31] to RL, showing linear weight soups can approximate Pareto fronts and reduce reward misspecification, yet multi-reward methods often underperform specialized single-reward experts. We therefore propose two *a posteriori* solutions, RaTE and MapReduce LoRA, to address reward conflict. Specifically, the iterative merging in MapReduce LoRA shares a technical spirit with periodic averaging in FedAvg [41] and DiLoCo [10]; however, while they focus on communication efficiency across GPU clusters, our work leverages this mechanism to navigate the Pareto front for multi-preference alignment.

3. Method

3.1. Preliminaries

Low-Rank Adaptation (LoRA) [15] is a leading parameter-efficient fine-tuning method that adapts large

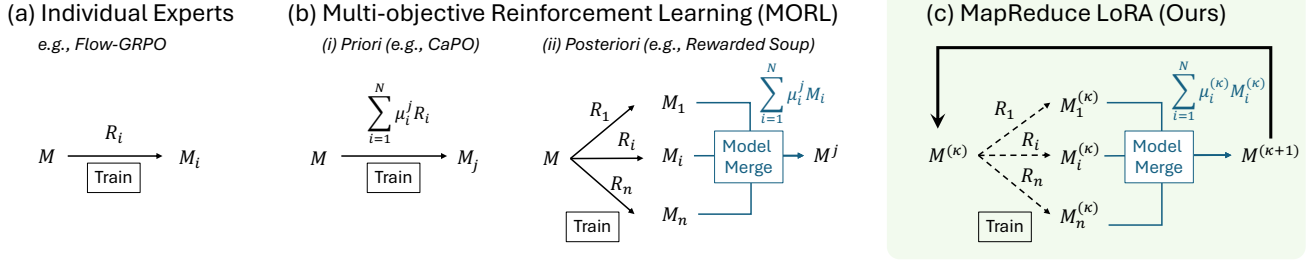


Figure 3. **Overview of MapReduce LoRA and comparison with (a) individual experts, e.g., Flow-GRPO [26], and (b) Multi-Objective Reinforcement Learning, e.g., CaPO [21] and Rewarded soup [36].** All methods begin from a base model M and optimize with respect to reward R . Our proposed MapReduce LoRA iteratively trains per-reward LoRA experts and initializes iteration $k + 1$ using the merged model from iteration k . Notably, the black dashed curve for MapReduce LoRA indicates fewer training steps compared with the black solid curves representing other methods.

models by learning a low-rank update to frozen pre-trained weights. For a linear layer with weight $W \in \mathbb{R}^{d \times k}$ and input x , the adapted layer is

$$(W + \Delta W)x = Wx + BAx, \quad \text{with } \Delta W = BA,$$

where $A \in \mathbb{R}^{r \times k}$, $B \in \mathbb{R}^{d \times r}$, and $r \ll \min(d, k)$. During fine-tuning, W remains fixed while only A and B are trained, optionally scaled by a factor α/r ; at inference, ΔW can be merged into W . Recent work [37] finds that, in common post-training settings (small/medium-scale SFT, reasoning, or RL), LoRA matches full fine-tuning performance when rank and layer coverage suffice. LoRA has been used for style [48] and skill control [23], but multi-preference control remains underexplored; we therefore study LoRA merging for multi-preference optimization.

Textual Inversion [13] learns a new embedding vector for a pseudo-token that represents a specific concept. Given only three to five reference images, it optimizes a single token embedding to encode both the high-level semantics and the fine-grained visual details of the concept, enabling personalized and reference-guided generation without modifying the base model.

Pareto Fronts (PF) [33] represents the collection of non-dominated solutions, model parameters for which no other candidate can improve one objective without degrading another. Formally, $\text{PF} = \{\theta \mid \nexists \theta' \in \Theta, \{R_i(\theta')\}_i \succ_{\mathbb{R}^N} \{R_i(\theta)\}_i\}$, where $\succ_{\mathbb{R}^N}$ denotes the dominance relation in the N -dimensional reward space indexed by i , and N denotes the total number of reward objectives.

Group Relative Policy Optimization (GRPO) [26, 39, 45] is a PPO-style preference optimization algorithm but based on group-normalized rewards. For each prompt p , GRPO samples G results $\{y^g\}_{g=1}^G$ and computes group-normalized advantages \hat{A}^g by z-scoring rewards within that group as shown in Eqn. (2). The policy is then updated with a clipped

likelihood-ratio objective and regularized by a KL penalty w.r.t a frozen reference policy as shown in Eqn. (1).

$$\mathcal{J}_{\text{GRPO}} = \mathbb{E}_p \left[\frac{1}{G} \sum_{g=1}^G \frac{1}{T} \sum_{t=1}^T \min(r_t^g \hat{A}^g, \text{clip}(r_t^g, 1 - \epsilon, 1 + \epsilon) \hat{A}^g) \right] - \beta D_{\text{KL}}(\pi_\theta(\cdot | p) \| \pi_{\text{ref}}(\cdot | p)), \quad (1)$$

$$\hat{A}^g = \frac{R(y^g, p) - \text{mean}[R(y^g, p)]_{g=1}^G}{\text{std}[R(y^g, p)]_{g=1}^G}. \quad (2)$$

3.2. MapReduce LoRA

In this section, we first demonstrate that MapReduce is a progressive souping process via averaged proximal consensus optimization. Then, we prove that MapReduce progressively converges toward the joint optimum of the conditions set by multiple reward models. Finally, we explain why MapReduce outperforms the one-shot soup method [36]. Fig. 3 shows the overview of MapReduce LoRA and a comparison with individual experts and multi-objective reinforcement learning [21, 36].

Let $\{f_i(\theta)\}_{i=1}^n$ denote differentiable reward objectives, each derived from a distinct reward model used in GRPO [39] fine-tuning. The joint optimization goal is to maximize their average:

$$F(\theta) = \frac{1}{n} \sum_{i=1}^n f_i(\theta), \quad (3)$$

where $\theta \in \mathbb{R}^d$ are model parameters of the diffusion model.

MapReduce is implemented by iteratively optimizing multiple reward functions for a few steps and averaging the resulting weights, a process we formalize as progressive

souping. At iteration k :

$$\begin{aligned}\theta_i^k &= \text{prox}_{\eta f_i}(\theta^k) = \arg \max_{\theta} (f_i(\theta) - \frac{1}{2\eta} \|\theta - \theta^k\|^2), \\ \theta^{k+1} &= \frac{1}{n} \sum_{i=1}^n \theta_i^k,\end{aligned}\quad (4)$$

where the proximal term $\frac{1}{2\eta} \|\theta - \theta^k\|^2$ corresponds to a trust region in GRPO. The overall operator can be written as:

$$T(\theta) = \frac{1}{n} \sum_{i=1}^n \text{prox}_{\eta f_i}(\theta). \quad (5)$$

Thus, progressive souping performs repeated applications of the averaged proximal map $\theta^{k+1} = T(\theta^k)$, while a one-shot ‘‘final soup’’ corresponds to a single application $T(\theta^0)$.

Now we prove that MapReduce progressively reaches the optimum of Eqn. (3). Because the sampling distribution p_{θ} of a pretrained diffusion model changes smoothly with θ (the score function $\nabla_{\theta} \log(p_{\theta})$ is continuous), we can safely assume that each reward objective $f_i(\theta)$ is locally \mathcal{L} -smooth and the aggregated objective Eqn. (3) satisfies the Polyak–Łojasiewicz (PL) condition in a neighborhood containing the optimization trajectory:

$$\frac{1}{2} \|\nabla F(\theta)\|^2 \geq \mu \|F(\theta) - F^*\|, \quad (6)$$

for some constant $\mu > 0$. Then, for step size $0 < \eta \leq 1/\mathcal{L}$, each proximal operator $\text{prox}_{\eta f_i}(\theta)$ is nonexpansive in a local neighborhood, and the overall operator $T(\theta)$ is thus an α -averaged operator. The fixed points of $T(\theta)$ coincide with the stationary points of the aggregated objective $\nabla F(\theta^*) = 0$. The progressive-soup iteration in Eqn. (4) converges to a stationary point of Eqn. (3) and satisfies the geometric contraction bound:

$$\|F(\theta^{k+1}) - F^*\| \leq (1 - c\eta\mu) \|F(\theta^k) - F^*\|, \quad (7)$$

for some constant $c \in (0, 1)$.

A one-shot final soup performs a single application of T ; progressive souping applies T repeatedly, resulting in a smaller sub-optimality gap:

$$\|F(\theta^m) - F^*\| \leq (1 - c\eta\mu)^m \|F(\theta^0) - F^*\|, \quad (8)$$

where m denotes the iteration. Hence, each progressive-soup iteration further contracts toward the joint optimum, while the one-shot soup remains suboptimal unless initialized near a stationary point. The comparison between progressive souping and one-shot soup is shown in Figs. 1, 2 and 4. *Please refer to the Supplement B for the pseudocode.*

3.3. Reward-aware Token Embedding (RaTE)

We propose RaTE to make the token embedding sensitive to user preferences and dynamically control inference-time

reward influences. Inspired by Textual Inversion [13], we distill each preference into a single, trainable special token embedding via supervised fine-tuning. Both teacher and student share the same frozen Transformer backbone M . We detail the setup below.

- **Teacher:** For each preference i , we attach its expert LoRA adapter θ_i to M . This teacher produces the target latent $z_{0,i}^{\text{teacher}}$ for the i -th preference.
- **Student:** The student is the frozen M without adapters. Its prompt includes the i -th special token; the token embedding θ_{token_i} is the only trainable parameter.

We distill θ_i into θ_{token_i} using a Flow Matching objective [25]. Sample t via a flow-matching timestep schedule (e.g., logit-normal or uniform (depending on the scheduler/model)), sample $\epsilon \sim \mathcal{N}(0, I)$, and set $z_t = (1 - \sigma_t) z_{0,i}^{\text{teacher}} + \sigma_t \epsilon$, where σ_t is given by the scheduler. The student M predicts the velocity from z_t and the conditioned prompt $c(p, \theta_{\text{token}_i})$. The target velocity is $v_{\text{target}} = \epsilon - z_{0,i}^{\text{teacher}}$. The loss minimizes the Mean Squared Error (MSE) between prediction and target, updating only θ_{token_i} :

$$\mathcal{L}(\theta_{\text{token}_i}) = \mathbb{E}_{p, z_{0,i}^{\text{teacher}}, \epsilon, t} \left[\left\| M(z_t, t, c(p, \theta_{\text{token}_i})) - v_{\text{target}} \right\|_2^2 \right]. \quad (9)$$

After training, we obtain the expert-infused token embedding θ_{token_i} . At inference, appending its special token to a prompt injects the desired preference. RaTE is lightweight and modular, enabling composable control with other customizations such as LoRA adapters.

4. Experiments

4.1. Experimental Setup

Models and datasets. For *Text-to-Image generation*, we use Stable Diffusion 3.5 Medium (SD 3.5 M) [2] and FLUX.1-dev [20] as base models. We adopt the same datasets as Flow-GRPO [26]: GenEval [14], PickScore [18], and OCR [8]. We compare against CaPo [21], Flow-GRPO individual experts [26], multi-objective RL with mixed data (MORL-D) and with mixed data plus mixed rewards (MORL-DR), and Rewarded Soup [36]. The merging iteration is 4 for all reported results if not specified. For *Text-to-Video generation*, we use the HunyuanVideo backbone [19]. We follow the Dance-GRPO [45] GitHub recipe (optimizer, GRPO grouping, scheduler, data sampling), but apply parameter-efficient LoRA instead of full fine-tuning. We compare to Dance-GRPO individual experts [45]. Because the GitHub configuration differs from the paper, we report reproduced baselines trained on the released data for fairness. The merging iteration is 3 for all reported results if not specified. For *Language tasks*, we use llama2-7B [42] as base model, following Bone Soup [44] setup. We first train the Llama2-7B [42] backbone via supervised fine-tuning (SFT) using

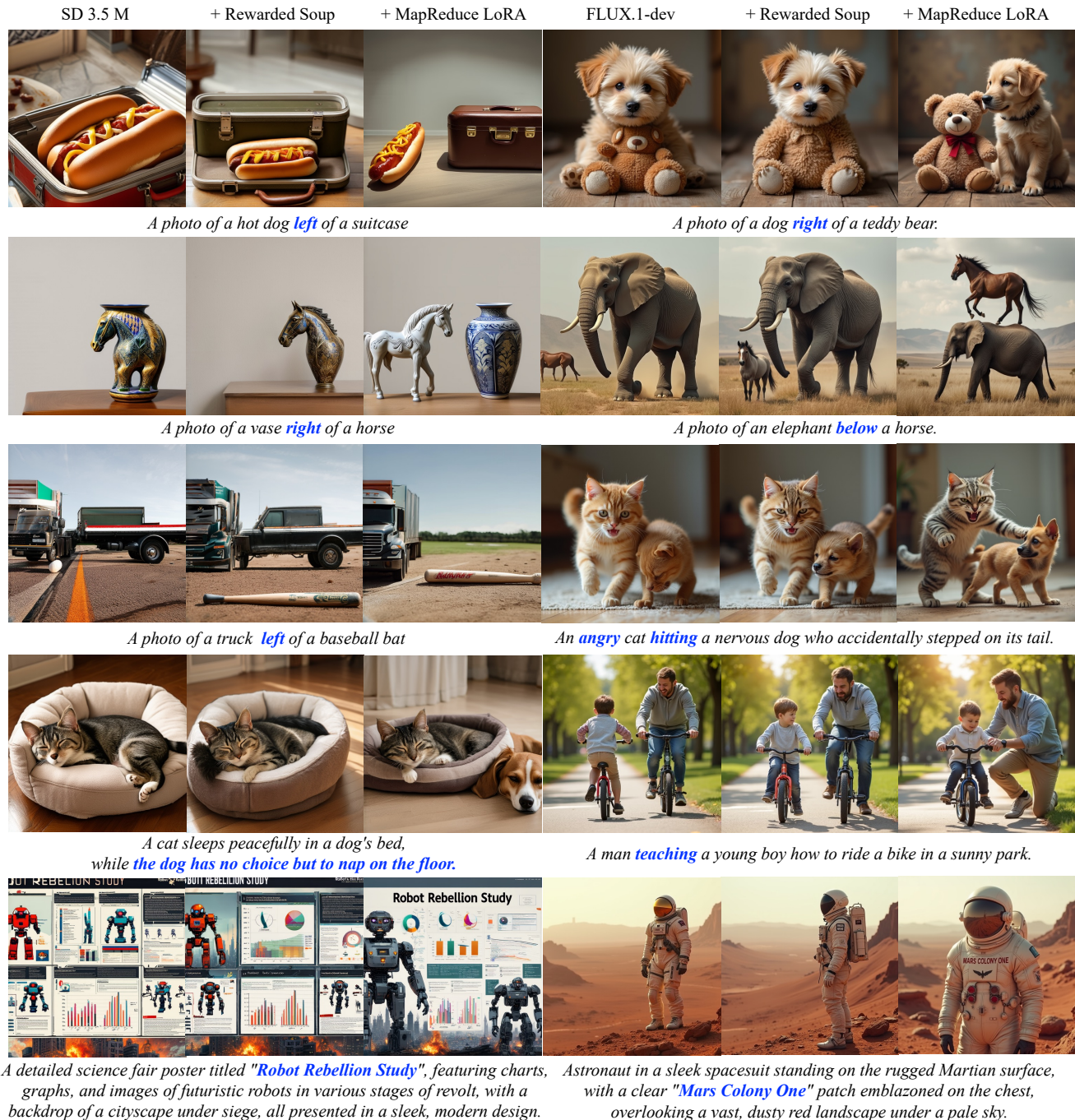


Figure 4. **MapReduce LoRA** enhances the generative qualities, *i.e.*, image aesthetics, positional relationship and text rendering quality, by optimizing the model with multiple rewards simultaneously.

the same datasets and hyperparameters as Bone Soup [44], then train LoRA experts with PPO [38] under the same settings of datasets and training hyperparameters. The merging iteration is 3 for all reported results if not specified. *For implementation details, please refer to the Supplement C.*

Reward models. For *Text-to-Image*, we train with three rewards: detection-based text-image alignment

(GenEval [14]), human preference (PickScore [18]), and text rendering quality (OCR [8]). For evaluation, we additionally report clip-based text-image alignment (VQAScore [24]), human preference (MPS [47]), and aesthetic quality (VILA [17]). For *Text-to-Video*, we use two rewards: Visual Quality (VQ) and Motion Quality (MQ) from VideoAlign [27]. For the *Language* task, we employ four

Table 1. Text-to-Image performance comparison on in-domain rewards (GenEval [14], PickScore [18], and OCR [8]) within corresponding datasets and out-of-domain rewards (VQAScore [24], MPS [47], and VILA [17]) within PartiPrompts [46] and GenAI-Bench [22]. *The performance is evaluated with fp32 precision. Red color means the performance is degraded compared to the baseline.*

Method	Reward	GenEval [14]							PickScore	OCR	PartiPrompts			GenAIBench
		Single Obj.	Two Obj.	Counting	Colors	Position	Color Attr.	Overall			VQAScore	MPS	VILA	VQAScore
SD 3 M* [3]	x	0.99	0.84	0.56	0.84	0.32	0.52	0.68	-	-	0.908	13.39	5.793	-
SD 3 M + CaPO* [21]	VQAScore [24]													
	+MPS [47]	0.99	0.87	0.63	0.86	0.31	0.59	0.71	-	-	0.914	13.58	5.943	-
	+VILA [17]	(+0.00%)	(+3.57%)	(+12.50%)	(+2.38%)	(-3.13%)	(+13.46%)	(+4.41%)	-	-	(+0.66%)	(+1.42%)	(+2.59%)	-
SD 3.5 M [2]	x	1.00	0.86	0.55	0.82	0.23	0.62	0.68	21.784	0.601	0.861	11.68	6.034	0.744
Individual Experts (Flow-GRPO [26])	GenEval [14]	1.00	0.96	0.93	0.91	0.93	0.84	0.93	21.852	0.654	0.879	11.81	6.101	0.782
	PickScore [18]	1.00	0.94	0.76	0.88	0.36	0.59	0.76	23.359	0.716	0.880	12.66	6.755	0.774
	OCR [8]	1.00	0.87	0.56	0.82	0.25	0.59	0.68	21.800	0.934	0.863	11.75	6.014	0.750
Rewardred Soup [36]	[14] + [18] + [8]	1.00	0.94	0.76	0.86	0.43	0.72	0.79	22.276	0.805	0.885	12.13	6.194	0.772
MORL-D ^α	[14] + [18] + [8]	1.00	0.99	0.94	0.89	0.88	0.78	0.91	22.067	0.942	0.881	12.00	6.113	0.777
MORL-DR ^α	[14] + [18] + [8]	1.00	0.82	0.61	0.81	0.21	0.59	0.67	21.834	0.641	0.860	11.71	6.014	0.746
MapReduce LoRA	[14] + [18] + [8]	1.00	0.98	0.93	0.88	0.81	0.78	0.90	22.552	0.923	0.885	12.25	6.266	0.782
		(+0.00%)	(+14.12%)	(+68.18%)	(+7.80%)	(+252.17%)	(+25.81%)	(+31.88%)	(+3.53%)	(+53.55%)	(+2.78%)	(+4.89%)	(+3.85%)	(+5.13%)
MapReduce LoRA + RaTE	[14] + [18] + [8]	1.00	0.98	0.93	0.90	0.95	0.79	0.92	22.777	0.936	0.877	12.44	7.238	0.777
		(+0.00%)	(+14.12%)	(+68.18%)	(+10.40%)	(+313.04%)	(+27.42%)	(+36.08%)	(+4.56%)	(+55.72%)	(+1.85%)	(+6.49%)	(+19.96%)	(+4.37%)
FLUX.1-dev [20]	x	0.99	0.87	0.71	0.82	0.18	0.44	0.67	22.006	0.573	0.830	12.37	6.629	0.737
Individual Experts (Flow-GRPO [26])	GenEval [14]	1.00	1.00	0.90	0.89	0.90	0.73	0.90	22.057	0.692	0.854	12.45	6.661	0.764
	PickScore [18]	1.00	0.95	0.61	0.85	0.24	0.57	0.70	23.566	0.723	0.875	12.76	5.514	0.772
	OCR [8]	1.00	0.84	0.76	0.83	0.20	0.46	0.68	21.997	0.971	0.841	12.32	6.591	0.749
Rewardred Soup [36]	[14] + [18] + [8]	0.99	0.96	0.81	0.88	0.31	0.66	0.77	22.503	0.868	0.862	12.73	6.650	0.767
MORL-D ^α	[14] + [18] + [8]	1.00	0.99	0.89	0.90	0.78	0.73	0.88	22.026	0.932	0.834	12.36	6.513	0.733
MORL-DR ^α	[14] + [18] + [8]	1.00	0.95	0.90	0.94	0.73	0.79	0.88	22.112	0.952	0.840	12.41	6.534	0.745
MapReduce LoRA	[14] + [18] + [8]	1.00	0.96	0.88	0.88	0.81	0.79	0.89	22.951	0.957	0.875	12.95	6.572	0.775
		(+1.27%)	(+10.46%)	(+22.81%)	(+7.80%)	(+350.00%)	(+79.55%)	(+32.68%)	(+4.29%)	(+67.06%)	(+5.49%)	(+4.70%)	(+0.87%)	(+5.09%)

* From CaPO Table 2 and 3 [21]; as the code is not released, we report their numbers and cannot compare CaPO on SD 3.5 M [2] and FLUX.1-dev [20].

^α The detailed settings of MORL-D/DR: Please refer to the Supplement C.

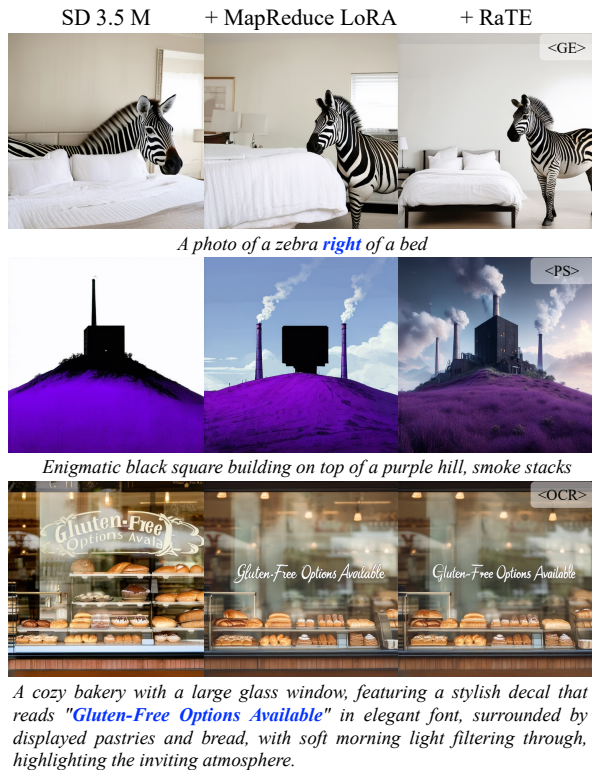


Figure 5. RaTE enables per-reward control at inference.

rewards across two tasks: Reddit Summary (Faithful and Preference1) and Helpful Assistant (Helpful and Harmless).

4.2. Qualitative Results

Fig. 2 shows iterative improvements from MapReduce LoRA and the controllability of RaTE (see also Fig. 5). Compared to the base model and Rewardred Soup [36] (Fig. 4), MapReduce LoRA better handles challenging cases, including uncommon spatial relations (e.g., an elephant below a horse) and high-quality rendering of small text. *For more qualitative results on Text-to-Image and Text-to-Video, please refer to the Supplement E.1 and E.2.*

4.3. Quantitative Results

MapReduce LoRA. Table 1 reports *Text-to-Image* performance on GenEval [14], PickScore [18], OCR [8], VQAScore [24], MPS [47], and VILA [17] using SD 3.5 M [2] and FLUX.1-dev [20]. MapReduce LoRA improves both in-domain and out-of-domain metrics. Relative to CaPO [21], it delivers larger gains across the four CaPO metrics. On CaPO’s in-domain metrics (VQAScore [24], MPS [47], VILA [17]), which are out-of-domain for us, our improvements are 2.78%, 4.89%, and 3.85%, exceeding CaPO’s 0.66%, 1.42%, and 2.59%. On CaPO’s out-of-domain metric (GenEval [14]), our improvement is 31.88% versus CaPO’s 4.41%. Flow-GRPO individual experts [26], each tuned to a single reward, substantially boost the tar-

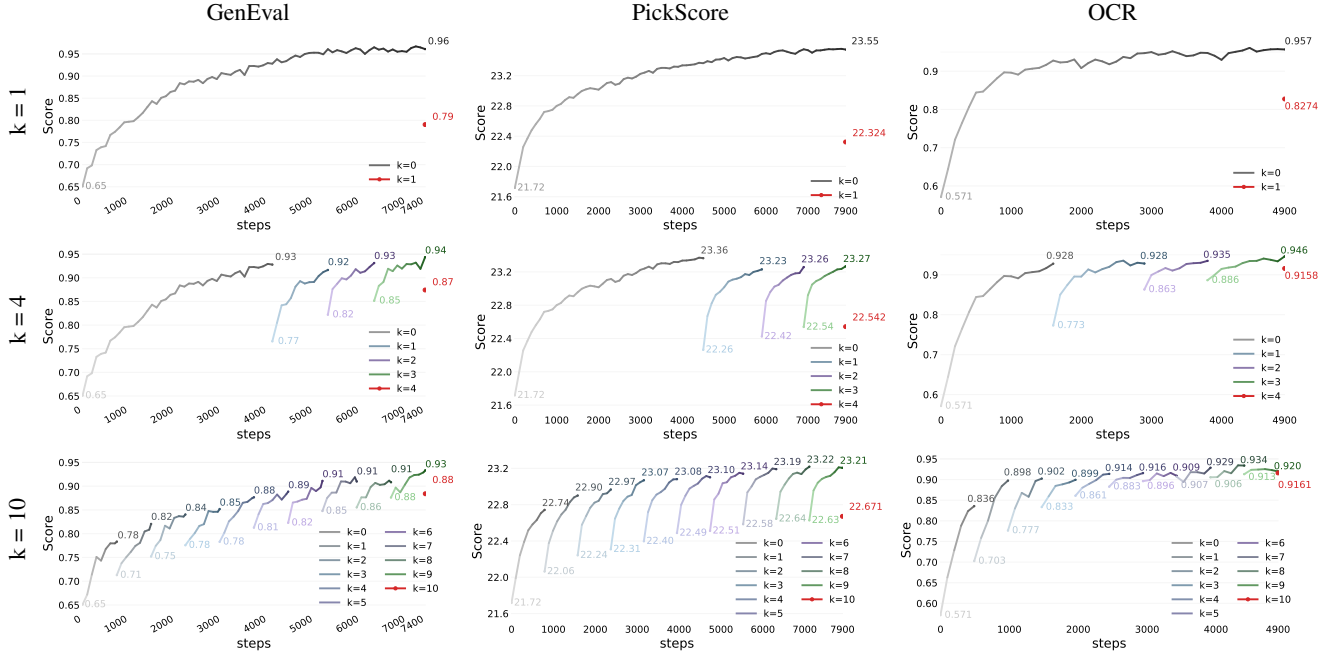


Figure 6. **Ablation study on merging iterations** ($k = 1$ vs. 4 vs. 10). The performance is evaluated during training with mixed precision, where the text encoder is set to *fp16* precision and the rest of the model to *fp32*.

geted metric but transfer poorly to others. MORL-D and MORL-DR can be unstable under conflicting objectives; for instance, PickScore often collapses during joint training and is dominated by other rewards (*e.g.*, OCR). In contrast, MapReduce LoRA maintains competitive performance across all targeted rewards.

Table 2 reports *Text-to-Video* results. We evaluate 1,024 held-out prompts (fixed once). For each prompt, we generate four samples using a fixed set of seeds shared across models and report mean Visual Quality (VQ) and Motion Quality (MQ) from VideoAlign [27]. MapReduce LoRA improves both VQ and MQ (+48.09% and +89.96%) over individually trained experts (+34.55% and +74.10%).

In Figs. 7 and 8, we compare MapReduce LoRA against Llama2 (base) [42], Llama2 after SFT, Rewarded Soup [36], and Bone Soup [44]. MapReduce LoRA achieves state-of-the-art performance on both tasks, underscoring its cross-modal generality.

Table 2. Text-to-Video comparison on Visual and Motion Quality.

Method	Reward	VQ	MQ
HunyuanVideo [19]	x	3.25	0.95
Individual Experts	VQ	4.37 (+34.55%)	1.20 (+26.41%)
(DanceGRPO [45])	MQ	3.80 (+16.95%)	1.66 (+74.10%)
Rewarded Soup [36]	VQ+MQ	4.13 (+27.37%)	1.43 (+50.42%)
MapReduce LoRA	VQ+MQ	4.81 (+48.09%)	1.81 (+89.96%)

[Ablation] MapReduce LoRA: Effect of merging iterations under a fixed training budget. With the total training steps fixed (Fig. 6), we compare merging iterations $k \in \{1, 4, 10\}$. Increasing k consistently improves final

performance and reduces degradation from merging multiple experts. For $k = 10$ relative to $k = 4$ and $k = 1$, the gains are +1.12% and +11.84% on GenEval [14], +0.57% and +1.56% on PickScore [18], and +0.03% and +10.72% on OCR [8].

Reward-aware token embedding (RaTE). Tables 1 and 3 report RaTE performance on GenEval [14], PickScore [18], and OCR [8] using SD 3.5 M [2]. At inference, RaTE appends a trained control token to the end of the prompt based on the specified preference. RaTE enables per-reward control and jointly improves multiple rewards. In Table 1, token gains are orthogonal to transformer tuning: RaTE adds 4.20%, 1.03%, and 2.17% on GenEval [14], PickScore [18], and OCR [8], respectively. In Table 3, when using all three tokens, the first appended token accounts for most of the gain. RaTE enables lightweight, composable inference-time control and costs only 0.1579 \times of MapReduce LoRA to train. Token control is effective on Stable Diffusion [2, 5, 13], which uses explicit cross-attention for text conditioning. In contrast, FLUX.1-dev [20] performs joint text-image sequence modeling, causing a modified token embedding to perturb both text and image tokens across layers, which makes reward-specific token control substantially less stable. We leave this for future exploration.

[Ablation] RaTE: Effect of appended token count. Table 4 reports RaTE performance as we vary the number of appended tokens. In the table, <RaTE> denotes the metric-specific token: <GE> for GenEval [14], <PS> for PickScore [18], and <OCR> for OCR [8]. Performance peaks differ by reward: GenEval saturates at 2–3 tokens (0.78), PickScore

Table 3. **Reward-aware Token Embedding results.** <GE>, <PS>, and <OCR> denote tokens trained on GenEval [14], PickScore [18], and OCR [8], respectively. Gray indicates not trained on that reward; **bold** indicates the best among variants.

Method	GenEval [14]	PickScore [18]	OCR [8]
SD 3.5 M [2]	0.68	21.784	0.601
+ <GE>	0.76	21.732	0.601
+ <PS>	0.69	22.052	0.591
+ <OCR>	0.68	21.724	0.623
+ <GE> + <PS>	0.77	21.990	0.610
+ <GE> + <OCR>	0.77	21.690	0.633
+ <PS> + <GE>	0.74	22.014	0.599
+ <PS> + <OCR>	0.69	22.064	0.592
+ <OCR> + <GE>	0.75	21.736	0.619
+ <OCR> + <PS>	0.69	22.040	0.607
+ <GE> + <PS> + <OCR>	0.76	21.992	0.613
+ <GE> + <OCR> + <PS>	0.75	21.981	0.615
+ <PS> + <GE> + <OCR>	0.75	22.009	0.606
+ <PS> + <OCR> + <GE>	0.72	22.027	0.606
+ <OCR> + <GE> + <PS>	0.73	22.013	0.617
+ <OCR> + <PS> + <GE>	0.74	22.014	0.614

peaks at 1 (22.052), and OCR peaks at 3 (0.635).

Table 4. Ablation on the number of appended RaTE tokens.

Method	GenEval [14]	PickScore [18]	OCR [8]
SD 3.5 M [2]	0.68	21.784	0.601
+ <RaTE> x1	0.76	22.052	0.623
+ <RaTE> x2	0.78	22.037	0.621
+ <RaTE> x3	0.78	22.021	0.635
+ <RaTE> x10	0.78	21.993	0.630

5. Conclusion

We present MapReduce LoRA and RaTE, two complementary methods to address the "alignment tax" in multi-preference post-training. By iteratively merging parallel reward experts and distilling them into composable token embeddings, our framework converts objective trade-offs into a controllable tuning strategy. Extensive evaluations across text-to-image (SD 3.5, FLUX.1), video (HunyuanVideo), and language (Llama-2) models demonstrate substantial gains in both targeted and untargeted metrics. Overall, our approach offers a simple, scalable recipe for systematically advancing the multi-preference Pareto front and enabling practical model customization.

6. Acknowledgment

We appreciate the valuable suggestions provided by Tsung-Han Wu, Yu-Heng Hung, Fengzhe Zhou, and Jitesh Jain for this paper. This research was supported in part by the National Science Foundation under Award #2427478 - CAREER Program, and by the National Science Foundation and the Institute of Education Sciences, U.S. Department of Education under Award #2229873 - National AI Institute for Exceptional Education. This project was also partially supported by cyberinfrastructure resources and services provided by College of Computing at the Georgia Institute of Technology, Atlanta, Georgia, USA.

References

- [1] Akhil Agnihotri, Rahul Jain, Deepak Ramachandran, and Zheng Wen. Multi-objective preference optimization: Improving human alignment of generative models. *arXiv preprint arXiv:2505.10892*, 2025. 2, 3
- [2] Stability AI. Stable diffusion 3.5 medium. <https://huggingface.co/stabilityai/stable-diffusion-3.5-medium>, 2024. 1, 3, 5, 7, 8, 9, 15, 16, 17, 18
- [3] Stability AI. Stable diffusion 3 medium. <https://huggingface.co/stabilityai/stable-diffusion-3-medium>, 2024. 7
- [4] Kevin Black, Michael Janner, Yilun Du, Ilya Kostrikov, and Sergey Levine. Training diffusion models with reinforcement learning. In *Proceedings of the International Conference on Learning Representations (ICLR)*, 2024. 3
- [5] Chieh-Yun Chen, Chiang Tseng, Li-Wu Tsao, and Hong-Han Shuai. A cat is A cat (not A dog!): Unraveling information mix-ups in text-to-image encoders through causal analysis and embedding optimization. In *Advances in Neural Information Processing Systems (NeurIPS)*, 2024. 8
- [6] Chieh-Yun Chen, Min Shi, Gong Zhang, and Humphrey Shi. T2i-copilot: A training-free multi-agent text-to-image system for enhanced prompt interpretation and interactive generation. In *Proceedings of the IEEE/CVF International Conference on Computer Vision (ICCV)*, 2025. 3
- [7] Paul F. Christiano, Jan Leike, Tom B. Brown, Miljan Martic, Shane Legg, and Dario Amodei. Deep reinforcement learning from human preferences. In *Advances in Neural Information Processing Systems (NeurIPS)*, 2017. 3
- [8] Cheng Cui et al. Paddleocr 3.0 technical report, 2025. 1, 2, 3, 5, 6, 7, 8, 9, 15, 16, 19
- [9] Chaorui Deng, Deyao Zhu, Kunchang Li, Chenhui Gou, Feng Li, Zeyu Wang, Shu Zhong, Weihao Yu, Xiaonan Nie, Ziang Song, Shi Guang, and Haoqi Fan. Emerging properties in unified multimodal pretraining. *arXiv preprint arXiv:2505.14683*, 2025. 1, 3
- [10] Arthur Douillard, Qixiang Feng, Andrei A. Rusu, Rachita Chhaparia, Yani Donchev, Adhiguna Kuncoro, Marc’Aurelio Ranzato, Arthur Szlam, and Jiajun Shen. Diloco: Distributed low-communication training of language models. *arXiv preprint arXiv:2311.08105*, 2023. 3
- [11] Patrick Esser et al. Scaling rectified flow transformers for high-resolution image synthesis. In *Proceedings of the International Conference on Machine Learning (ICML)*, 2024. 1, 3
- [12] Jonathan Frankle, Gintare Karolina Dziugaite, Daniel M. Roy, and Michael Carbin. Linear mode connectivity and the lottery ticket hypothesis. In *Proceedings of the International Conference on Machine Learning (ICML)*, 2020. 3
- [13] Rinon Gal, Yuval Alaluf, Yuval Atzmon, Or Patashnik, Amit Haim Bermano, Gal Chechik, and Daniel Cohen-Or. An image is worth one word: Personalizing text-to-image generation using textual inversion. In *Proceedings of the In-*

- ternational Conference on Learning Representations (ICLR)*, 2023. 4, 5, 8
- [14] Dhruva Ghosh, Hannaneh Hajishirzi, and Ludwig Schmidt. Geneval: An object-focused framework for evaluating text-to-image alignment. In *Advances in Neural Information Processing Systems (NeurIPS)*, 2023. 1, 2, 3, 5, 6, 7, 8, 9, 15, 16, 19
- [15] Edward J. Hu, Yelong Shen, Phillip Wallis, Zeyuan Allen-Zhu, Yuanzhi Li, Shean Wang, Lu Wang, and Weizhu Chen. Lora: Low-rank adaptation of large language models. In *Proceedings of the International Conference on Learning Representations (ICLR)*, 2022. 3
- [16] Borja Ibarz, Jan Leike, Tobias Pohlen, Geoffrey Irving, Shane Legg, and Dario Amodei. Reward learning from human preferences and demonstrations in atari. In *Advances in Neural Information Processing Systems (NeurIPS)*, 2018. 3
- [17] Junjie Ke, Keren Ye, Jiahui Yu, Yonghui Wu, Peyman Milanfar, and Feng Yang. VILA: learning image aesthetics from user comments with vision-language pretraining. In *Proceedings of the IEEE/CVF Conference on Computer Vision and Pattern Recognition (CVPR)*, 2023. 2, 3, 6, 7, 16
- [18] Yuval Kirstain, Adam Polyak, Uriel Singer, Shahbuland Matiana, Joe Penna, and Omer Levy. Pick-a-pic: An open dataset of user preferences for text-to-image generation. In *Advances in Neural Information Processing Systems (NeurIPS)*, 2023. 1, 2, 3, 5, 6, 7, 8, 9, 15, 16, 19
- [19] Weijie Kong et al. HunyuanVideo: A systematic framework for large video generative models. *arXiv preprint arXiv:2412.03603*, 2024. 1, 3, 5, 8, 15, 16, 18, 25
- [20] Black Forest Labs. FLUX. <https://github.com/black-forest-labs/flux>, 2024. 1, 3, 5, 7, 8, 15, 16, 17, 18
- [21] Kyungmin Lee, Xiahong Li, Qifei Wang, Junfeng He, Junjie Ke, Ming-Hsuan Yang, Irfan Essa, Jinwoo Shin, Feng Yang, and Yinxiao Li. Calibrated multi-preference optimization for aligning diffusion models. In *Proceedings of the IEEE/CVF Conference on Computer Vision and Pattern Recognition (CVPR)*, 2025. 2, 3, 4, 5, 7
- [22] Baiqi Li, Zhiqiu Lin, Deepak Pathak, Jiayao Emily Li, Xide Xia, Graham Neubig, Pengchuan Zhang, and Deva Ramanan. GenAI-bench: A holistic benchmark for compositional text-to-visual generation. In *Synthetic Data for Computer Vision Workshop @ CVPR*, 2024. 7
- [23] Jialu Li, Jaemin Cho, Yi-Lin Sung, Jaehong Yoon, and Mohit Bansal. SELMA: learning and merging skill-specific text-to-image experts with auto-generated data. In *Advances in Neural Information Processing Systems (NeurIPS)*, 2024. 2, 3, 4
- [24] Zhiqiu Lin, Deepak Pathak, Baiqi Li, Jiayao Li, Xide Xia, Graham Neubig, Pengchuan Zhang, and Deva Ramanan. Evaluating text-to-visual generation with image-to-text generation. In *Proceedings of the European Conference on Computer Vision (ECCV)*, 2024. 2, 3, 6, 7, 16, 18
- [25] Yaron Lipman, Ricky T. Q. Chen, Heli Ben-Hamu, Maximilian Nickel, and Matthew Le. Flow matching for generative modeling. In *Proceedings of the International Conference on Learning Representations (ICLR)*, 2023. 1, 3, 5
- [26] Jie Liu, Gongye Liu, Jiajun Liang, Yangguang Li, Jiaheng Liu, Xintao Wang, Pengfei Wan, Di Zhang, and Wanli Ouyang. Flow-grpo: Training flow matching models via online RL. *arXiv preprint arXiv:2505.05470*, 2025. 1, 2, 3, 4, 5, 7, 15, 19
- [27] Jie Liu, Gongye Liu, Jiajun Liang, Ziyang Yuan, Xiaokun Liu, Mingwu Zheng, Xiele Wu, Qiulin Wang, Wenyu Qin, Menghan Xia, Xintao Wang, Xiaohong Liu, Fei Yang, Pengfei Wan, Di Zhang, Kun Gai, Yujie Yang, and Wanli Ouyang. Improving video generation with human feedback. *arXiv preprint arXiv:2501.13918*, 2025. 6, 8, 16
- [28] Xingchao Liu, Chengyue Gong, and Qiang Liu. Flow straight and fast: Learning to generate and transfer data with rectified flow. In *Proceedings of the International Conference on Learning Representations (ICLR)*, 2023. 1, 3
- [29] Ilya Loshchilov and Frank Hutter. Decoupled weight decay regularization. In *Proceedings of the International Conference on Learning Representations (ICLR)*, 2019. 15
- [30] Yuhang Ma, Yunhao Shui, Xiaoshi Wu, Keqiang Sun, and Hongsheng Li. Hpsv3: Towards wide-spectrum human preference score. *arXiv preprint arXiv:2508.03789*, 2025. 2
- [31] Behnam Neyshabur, Hanie Sedghi, and Chiyuan Zhang. What is being transferred in transfer learning? In *Advances in Neural Information Processing Systems (NeurIPS)*, 2020. 3
- [32] Long Ouyang et al. Training language models to follow instructions with human feedback. In *Advances in Neural Information Processing Systems (NeurIPS)*, 2022. 3
- [33] Vilfredo Pareto. *Cours d'économie politique*. F. Rouge, 1896. 4
- [34] Adam Polyak et al. Movie Gen: A cast of media foundation models. *arXiv preprint arXiv:2410.13720*, 2024. 1, 3
- [35] Rafael Rafailov, Archit Sharma, Eric Mitchell, Christopher D. Manning, Stefano Ermon, and Chelsea Finn. Direct preference optimization: Your language model is secretly a reward model. In *Advances in Neural Information Processing Systems (NeurIPS)*, 2023. 1, 3
- [36] Alexandre Ramé, Guillaume Couairon, Corentin Dancette, Jean-Baptiste Gaya, Mustafa Shukor, Laure Soulier, and Matthieu Cord. Rewarded soups: towards pareto-optimal alignment by interpolating weights fine-tuned on diverse rewards. In *Advances in Neural Information Processing Systems (NeurIPS)*, 2023. 2, 3, 4, 5, 7, 8, 13, 17, 18, 19, 25
- [37] John Schulman and Thinking Machines Lab. Lora without regret. *Thinking Machines Lab: Connectionism*, 2025. <https://thinkingmachines.ai/blog/lora/>. 4
- [38] John Schulman, Filip Wolski, Prafulla Dhariwal, Alec Radford, and Oleg Klimov. Proximal policy optimization algorithms. *arXiv preprint arXiv:1707.06347*, 2017. 1, 3, 6, 13
- [39] Zhihong Shao, Peiyi Wang, Qihao Zhu, Runxin Xu, Junxiao Song, Mingchuan Zhang, Y. K. Li, Y. Wu, and Daya Guo. Deepseekmath: Pushing the limits of mathematical reasoning in open language models. *arXiv preprint arXiv:2402.03300*, 2024. 3, 4, 15
- [40] Nisan Stiennon, Long Ouyang, Jeff Wu, Daniel M. Ziegler, Ryan Lowe, Chelsea Voss, Alec Radford, Dario Amodei, and Paul F. Christiano. Learning to summarize from human feedback. *arXiv preprint arXiv:2009.01325*, 2020. 3

- [41] Tao Sun, Dongsheng Li, and Bao Wang. Decentralized federated averaging. *IEEE Trans. Pattern Anal. Mach. Intell.*, 2023. [3](#)
- [42] Hugo Touvron et al. Llama 2: Open foundation and fine-tuned chat models. *arXiv preprint arXiv:2307.09288*, 2023. [1](#), [3](#), [5](#), [8](#), [13](#)
- [43] Ang Wang et al. Wan: Open and advanced large-scale video generative models. *arXiv preprint arXiv:2503.20314*, 2025. [1](#), [3](#)
- [44] Guofu Xie, Xiao Zhang, Ting Yao, and Yunsheng Shi. Bone soups: A seek-and-soup model merging approach for controllable multi-objective generation. In *Proceedings of the Association for Computational Linguistics (ACL)*, 2025. [1](#), [5](#), [6](#), [8](#), [13](#)
- [45] Zeyue Xue, Jie Wu, Yu Gao, Fangyuan Kong, Lingting Zhu, Mengzhao Chen, Zhiheng Liu, Wei Liu, Qiushan Guo, Weilin Huang, and Ping Luo. DanceGRPO: Unleashing GRPO on visual generation. *arXiv preprint arXiv:2505.07818*, 2025. [1](#), [2](#), [3](#), [4](#), [5](#), [8](#), [15](#)
- [46] Jiahui Yu, Yuanzhong Xu, Jing Yu Koh, Thang Luong, Gunjan Baid, Zirui Wang, Vijay Vasudevan, Alexander Ku, et al. Scaling autoregressive models for content-rich text-to-image generation. *Transactions on Machine Learning Research (TMLR)*, 2022. [7](#)
- [47] Sixian Zhang, Bohan Wang, Junqiang Wu, Yan Li, Tingting Gao, Di Zhang, and Zhongyuan Wang. Learning multi-dimensional human preference for text-to-image generation. In *Proceedings of the IEEE/CVF Conference on Computer Vision and Pattern Recognition (CVPR)*, 2024. [3](#), [6](#), [7](#), [16](#), [18](#)
- [48] Ming Zhong, Yelong Shen, Shuohang Wang, Yadong Lu, Yizhu Jiao, Siru Ouyang, Donghan Yu, Jiawei Han, and Weizhu Chen. Multi-lora composition for image generation. *Transactions on Machine Learning Research (TMLR)*, 2024. [4](#)

Supplementary Materials

A. MapReduce LoRA on Language Tasks	13
B. Pseudocode	14
B.1. Train: MapReduce LoRA	14
B.2. Train: Reward-aware Token Embedding	14
B.3. Inference with MapReduce LoRA and RaTE	15
C. Implementation Details	15
C.1. Training Configuration	15
C.2. Base Models and Reward Models	16
D. More Quantitative Results	16
D.1. Full Results of Different Merging Ratios (Corresponding to Fig. 1)	16
D.2. Pareto Front Comparison of MORL vs. MapReduce LoRA	17
D.3. Scalability of Reward Numbers	18
E. More Qualitative Results	19
E.1. Text-to-Image qualitative results	19
E.2. Text-to-Video qualitative results	25
F. Limitations and Future Works	28

A. MapReduce LoRA on Language Tasks

Beyond Text-to-Image and Text-to-Video, we evaluate MapReduce LoRA on language tasks to demonstrate cross-modal generality. Following the Bone Soup [44] setup, we consider two tasks, each with two rewards: (i) Reddit Summary (Faithful, Preference1) and (ii) Helpful Assistant (Helpful, Harmless). We first train the Llama2-7B [42] backbone via supervised fine-tuning (SFT) using the same datasets and hyperparameters as Bone Soup [44], then train LoRA experts with PPO [38] under the same settings of datasets and training hyperparameters. In Figs. 7 and 8, we compare MapReduce LoRA against Llama2 (base) [42], Llama2 after SFT, Rewarded Soup [36], and Bone Soup [44]. MapReduce LoRA achieves state-of-the-art performance on both tasks, underscoring its cross-modal generality.

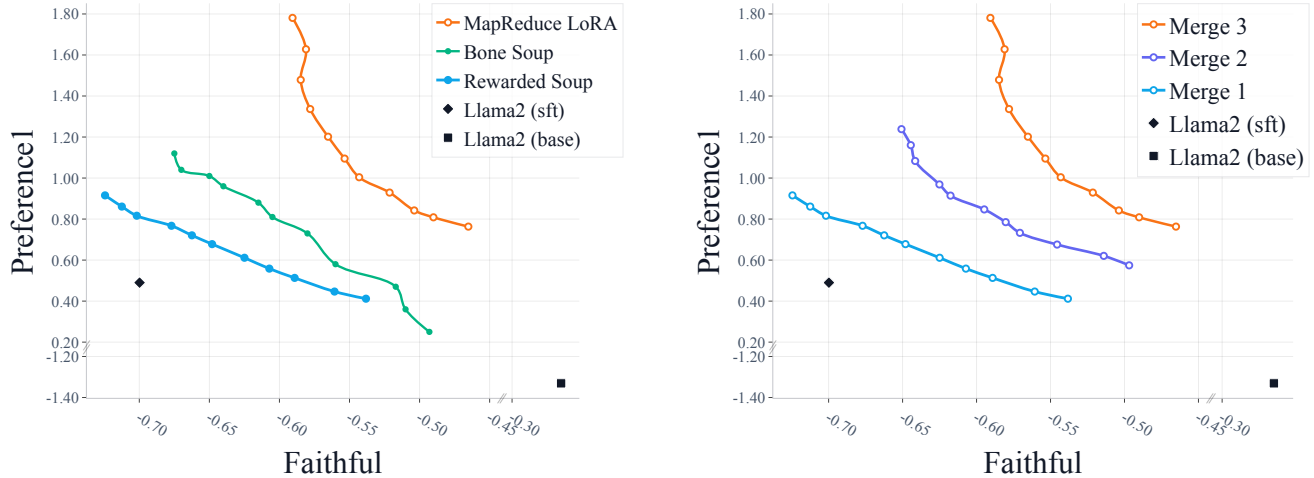


Figure 7. **Language Task: Reddit Summary.** Left: MapReduce LoRA outperforms Rewarded Soup [36] and Bone Soup [44] (reproduced from Fig. 5(c) in [44]) on both rewards. Right: MapReduce LoRA improves progressively across merge iterations.

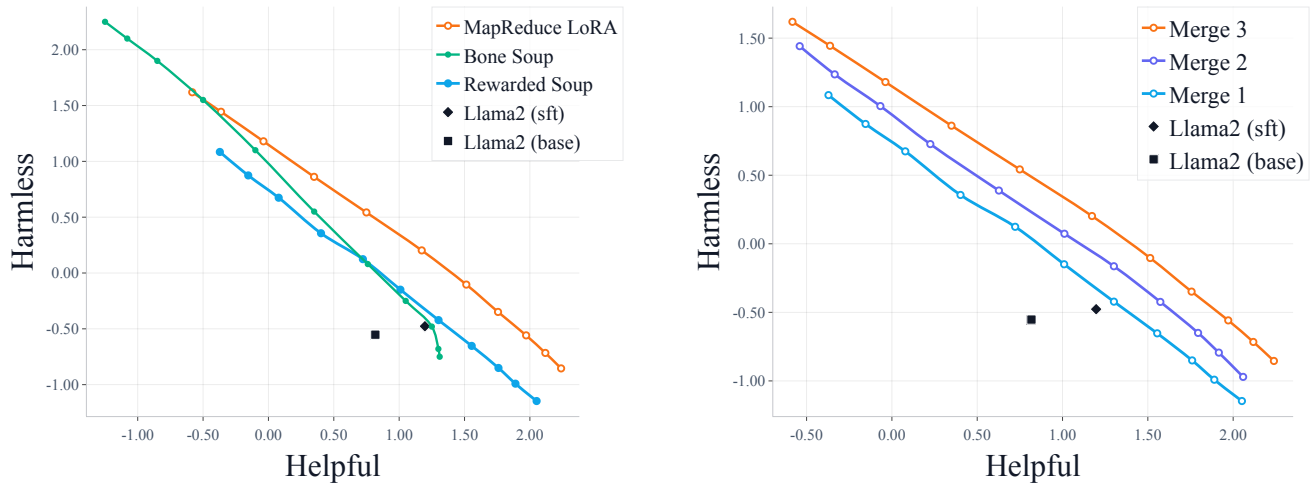


Figure 8. **Language Task: Helpful Assistant.** Left: MapReduce LoRA outperforms Rewarded Soup [36] and Bone Soup [44] (reproduced from Fig. 5(a) in [44]) on both rewards. Right: MapReduce LoRA improves progressively across merging iterations.

B. Pseudocode

B.1. Train: MapReduce LoRA

Algorithm 1 MapReduce LoRA: Multi-Preference Training

Require: Base model M with parameters $\theta^{(0)}$; Reward models $\{R_i\}_{i=1}^n$; LoRA configuration (target layers, rank r , scale α); Number of iterations K ; GRPO steps T_{GRPO} ; Merge weights $\{\mu_i\}_{i=1}^n$ (default $\mu_i = 1/n$, s.t. $\mu_i \geq 0$ and $\sum_{i=1}^n \mu_i = 1$); GRPO hyperparameters: Group size G , Clip ϵ , KL weight β

Ensure: Multi-preference aligned model $M^{(K)}$

- 1: Initialize reference policy $\pi_{\text{ref}} \leftarrow M(\theta^{(0)})$
- 2: **for** $k = 0$ to $K - 1$ **do**
- 3: **for all** $i \in \{1, \dots, n\}$ **do** ▷ Map phase: train per-reward LoRA experts in parallel
- 4: Initialize LoRA adapter $\phi_i^{(k)}$
- 5: Freeze base weights $\theta^{(k)}$; only $\phi_i^{(k)}$ is trainable
- 6: **for** $t = 1$ to T_{GRPO} **do**
- 7: $\phi_i^{(k)} \leftarrow \text{GRPO}(M, \theta^{(k)}, \phi_i^{(k)}, R_i, \pi_{\text{ref}}, G, \epsilon, \beta)$
- 8: **end for**
- 9: **end for**
- 10: $\bar{\phi}^{(k)} \leftarrow \sum_{i=1}^n \mu_i \phi_i^{(k)}$ ▷ Reduce phase: average experts
- 11: $\theta^{(k+1)} \leftarrow \text{MergeLoRAIntoBase}(\theta^{(k)}, \bar{\phi}^{(k)})$ ▷ update base model
- 12: $M \leftarrow M(\theta^{(k+1)})$
- 13: Reset all adapters $\phi_i^{(k)}$ to zero
- 14: Set $\pi_{\text{ref}} \leftarrow M(\theta^{(k+1)})$
- 15: **end for**
- 16: **return** $M^{(K)}$

B.2. Train: Reward-aware Token Embedding

Algorithm 2 Reward-aware Token Embedding (RaTE) Training

Require: Frozen base model M with parameters θ ; per-reward LoRA expert ϕ_i (teacher) for reward R_i ; training prompts \mathcal{D} ; special token index RaTE_i for reward i ; number of RaTE steps T_{RaTE} ; Flow Matching noise schedule $\{\sigma_t\}$

Ensure: Trained token embedding θ_i^{token} for reward i

- 1: Attach LoRA expert ϕ_i to M to form teacher model M_{teacher}
- 2: Freeze all Transformer weights and all token embeddings except θ_i^{token}
- 3: **for** $t = 1$ to T_{RaTE} **do**
- 4: Sample a minibatch of prompts $\{p_b\}_{b=1}^B$ from \mathcal{D}
- 5: **for each** prompt p in $\{p_b\}$ **do**
- 6: // **Teacher: obtain preference-specific latent**
- 7: Sample initial noise $\epsilon_0 \sim \mathcal{N}(0, I)$
- 8: Generate teacher latent $z_{0,i}^{\text{teacher}} \leftarrow \text{SAMPLE}(M_{\text{teacher}}, p, \epsilon_0)$
- 9: // **Flow Matching distillation setup**
- 10: Sample t via a flow-matching schedule (e.g., logit-normal over timesteps); sample $\epsilon \sim \mathcal{N}(0, I)$
- 11: Compute σ_t from the scheduler
- 12: $z_t \leftarrow (1 - \sigma_t) z_{0,i}^{\text{teacher}} + \sigma_t \epsilon$
- 13: Target velocity: $v_{\text{target}} \leftarrow \epsilon - z_{0,i}^{\text{teacher}}$
- 14: // **Student: base model + special token**
- 15: Construct prompt: $p' = \text{Concat}(p, \langle \text{RaTE}_i \rangle)$
- 16: Student velocity prediction: $v_{\text{pred}} \leftarrow M(z_t, t, c(p', \theta_i^{\text{token}}))$
- 17: Loss: $\mathcal{L}_{\text{RaTE}} \leftarrow \|v_{\text{pred}} - v_{\text{target}}\|_2^2$
- 18: Backpropagate and update only θ_i^{token} : $\theta_i^{\text{token}} \leftarrow \theta_i^{\text{token}} - \eta_{\text{RaTE}} \nabla_{\theta_i^{\text{token}}} \mathcal{L}_{\text{RaTE}}$
- 19: **end for**
- 20: **end for**
- 21: **return** θ_i^{token}

B.3. Inference with MapReduce LoRA and RaTE

Algorithm 3 Inference with MapReduce LoRA and RaTE

Require: Final merged model $M^{(K)}$ with parameters $\theta^{(K)}$; reward-aware tokens $\{<RaTE_i>\}$ and embeddings $\{\theta_i^{\text{token}}\}$; user prompt p ; user-specified preference set $\mathcal{S} \subseteq \{1, \dots, n\}$; sampling hyperparameters (number of steps, seeds, guidance scale, etc.)

Ensure: Generated image or video sample x

- 1: Build preference-aware prompt:
 - 2: $p^* \leftarrow p$
 - 3: **for** each $i \in \mathcal{S}$ in user-defined order **do**
 - 4: Append control token: $p^* \leftarrow \text{Concat}(p^*, <RaTE_i>)$
 - 5: **end for**
 - 6: Sample initial noise (image or video latent) $\epsilon_0 \sim \mathcal{N}(0, I)$
 - 7: Run the sampler with $M^{(K)}$ conditioned on p^* :
 - 8: $x \leftarrow \text{SAMPLE}(M^{(K)}, p^*, \epsilon_0)$
 - 9: **return** x
-

C. Implementation Details

C.1. Training Configuration

Reward-aware Token Embedding. For each reward-aware token embedding, it contains 3 embeddings corresponding to 3 text encoders within SD 3.5 M [2]. The embedding is trained on the GenEval, PickScore, and OCR datasets, individually. The teacher model is trained with LoRA via GRPO [39] with 4,200 steps on GenEval [14], 4,500 steps on PickScore [18] and 1,600 steps on OCR [8]. The training batchsize for GenEval is 512, PickScore is 768 and OCR is 768. We use the AdamW optimizer [29] with learning rate 3e-4, $\beta_1 = 0.9$, $\beta_2 = 0.999$, weight decay = 1e-4 and no warmup schedule; no KL penalty is applied.

MapReduce LoRA. We adopt uniform averaging for all the default experiments if not specified.

- **Text-to-Image:** We train all models using AdamW optimizer [29] with learning rate 3e-4, $\beta_1 = 0.9$, $\beta_2 = 0.999$, weight decay = 1e-4, and no warmup schedule. All experiments use 32 GPUs with global batch size 576.
 - **SD 3.5 M [2]:** We follow the training configuration in Flow-GRPO [26], where only the KL ratio β is different. $\beta_{\text{GenEval}} = 0.04$, $\beta_{\text{PickScore}} = 0.01$, and $\beta_{\text{OCR}} = 0.04$. The sampling timestep T is 10 and the evaluation timestep $T = 40$. The GRPO group size G is 24, the resolution is 512, and the LoRA settings are $\alpha = 64$ and $r = 32$. LoRA is applied to all attention layers (`attn.add_q_proj`, `attn.add_k_proj`, `attn.add_v_proj`, `attn.to_add_out`, `attn.to_q`, `attn.to_k`, `attn.to_v`, `attn.to_out.0`). The per-GPU batch sizes are 6, 9, and 9 with gradient accumulation steps of 3, 2, and 2 for GenEval, PickScore, and OCR, respectively. We train GenEval, PickScore and OCR for $\{4,100, 1,200, 1,000, 1,100\}$, $\{4,500, 1,400, 1,000, 1,000\}$, and $\{1,600, 1,300, 900, 1,100\}$ steps, respectively; the bracketed numbers denote merge iterations 0-3.
 - **FLUX.1-dev [20]:** The only task-dependent change is the KL ratio β ($\beta_{\text{GenEval}}=0.04$, $\beta_{\text{PickScore}}=0$, $\beta_{\text{OCR}}=0.04$). The sampling timestep T is 6 and the evaluation timestep $T = 28$. The GRPO group size G is 24, the resolution is 512, and the LoRA settings are $\alpha = 128$ and $r = 64$. LoRA is applied to attention layers and feed-forward network layers (`attn.to_q`, `attn.to_k`, `attn.to_v`, `attn.to_out.0`, `attn.add_q_proj`, `attn.add_k_proj`, `attn.add_v_proj`, `attn.to_add_out`, `ff.net.0.proj`, `ff.net.2`, `ff.context.net.0.proj`, `ff.context.net.2`). The per-GPU batch size is 3 with gradient accumulation steps of 6 for all three tasks. We train GenEval, PickScore and OCR for $\{2,700, 1,900, 1,800, 1,600\}$, $\{1,250, 600, 1,550, 2,200\}$, and $\{1,250, 650, 850, 1,100\}$ steps, respectively; the bracketed numbers denote merge iterations 0-3.
- **Text-to-Video:** We train the HunyuanVideo [19] with the same configuration as the DanceGRPO [45] but apply LoRA instead of full finetuning. The LoRA settings are $\alpha = 64$ and $r = 32$. LoRA is applied to attention layers “`attn.to_q`, `attn.to_k`, `attn.to_v`” in `single_transformer_blocks` (40 blocks), “`attn.to_q`, `attn.to_k`, `attn.to_v`, `attn.to_out.0`, `attn.to_add_out`, `attn.add_q_proj`, `attn.add_k_proj`, `attn.add_v_proj`” in `transformer_blocks` (20 blocks). We train VQ and MQ for $\{200, 140, 100\}$, $\{195, 145, 115\}$ steps, respectively; the bracketed numbers denote merge iterations 0-2.

Multi-objective Reinforcement Learning (MORL). The hyperparameters for MORL are identical to the MapReduce LoRA mentioned above. During each epoch, batches are sampled from GenEval [14], PickScore [18], and OCR [8] datasets according to specified ratios (default 1:1:1), where each individual batch contains samples from a single source. During evaluation, each data source is independently evaluated using its corresponding reward model to provide per-task performance metrics. The training steps are comparable to the overall training steps of MapReduce LoRA for fairness. There are two variations of MORL in our experiments, and the key difference lies in the data mixture and reward mixture strategy:

- **Data mixture (MORL-D)**: Each sample is only evaluated by its corresponding reward model based on its source dataset.
- **Data mixture and reward mixture (MORL-DR)**: Samples from GenEval [14] and OCR [8] are scored by both their task-specific reward and PickScore [18]; we take the average as the final reward (e.g., for GenEval, $(r_{\text{geneval}} + r_{\text{pickscore}})/2$). In contrast, samples from the PickScore dataset are evaluated only with PickScore. This choice reflects dataset constraints: GenEval requires a structured prompt format, whereas OCR requires prompts that contain text for a valid evaluation. PickScore serves as a shared aesthetic quality anchor across tasks. Overall, this protocol better aligns with the multi-objective setting by applying multiple rewards in a dataset-agnostic manner (where applicable), rather than restricting evaluation to dataset-specific rewards.

Compute Resources. All the experiments are conducted on 32 NVIDIA A100 GPUs (80GB).

C.2. Base Models and Reward Models

The following table presents the base model and reward models along with their corresponding links.

Models	Links
SD 3.5 M [2]	https://huggingface.co/stabilityai/stable-diffusion-3.5-medium
FLUX.1-dev [20]	https://huggingface.co/black-forest-labs/FLUX.1-dev
HunyuanVideo [19]	https://huggingface.co/hunyuanvideo-community/HunyuanVideo

Reward Models	Links
GenEval [14]	https://github.com/djghosh13/geneval
PickScore [18]	https://huggingface.co/yuvalkirstain/PickScore_v1
OCR [8]	https://github.com/PaddlePaddle/PaddleOCR
VQAScore [24]	https://github.com/linzhiqu/t2v_metrics
MPS [47]	https://github.com/Kwai-Kolors/MPS
VILA [17]	https://github.com/google-research/google-research/tree/master/vila
VQ and MQ [27]	https://github.com/KlingTeam/VideoAlign/tree/main

D. More Quantitative Results

D.1. Full Results of Different Merging Ratios (Corresponding to Fig. 1)

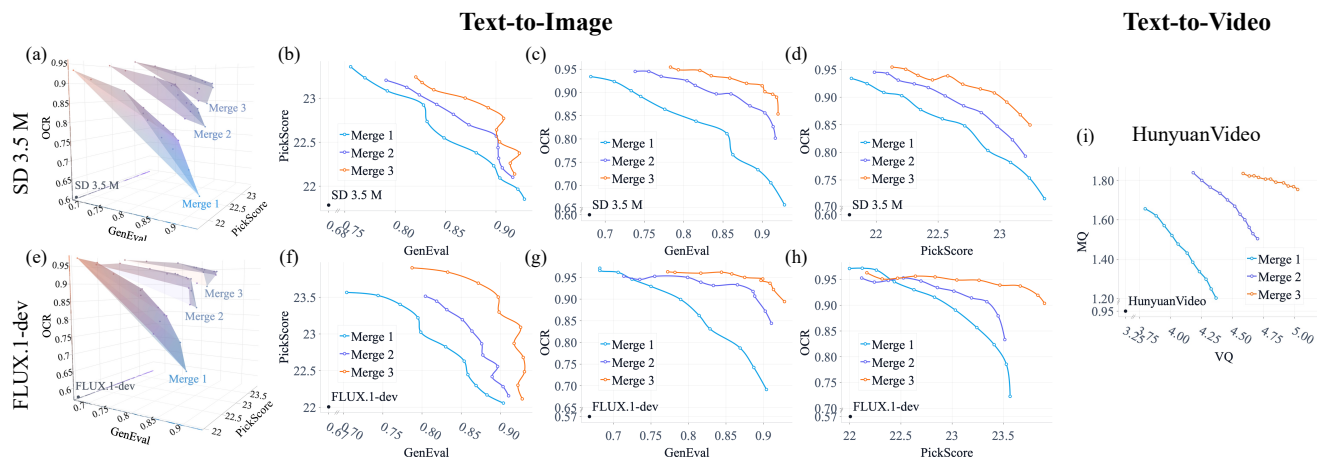


Figure 9. **MapReduce LoRA advances the Pareto fronts on Text-to-Image and Text-to-Video tasks.** We include the non-Pareto sets in this figure for sharing the full results.

Pareto fronts denote the set of non-dominated solutions (parameter settings for which no objective can be improved without degrading another). In Fig. 9, we include dominated (non-Pareto-optimal) points to present the full result set, together with the scores reported in Tables 5 and 6. Dominated points can arise for four reasons:

- **Estimation noise and stochasticity:** Each reward is estimated from finite samples and noisy reward evaluators. For GenEval, PickScore and OCR, we evaluate 553, 2,048 and 1,018 cases, respectively.
- **Non-convex objective landscapes:** The optimization surfaces can be highly non-convex. The merged model checkpoints may lie in different basins or apexes for different reward functions.
- **Partial or misaligned objectives:** When the two rewards are not orthogonal (*i.e.*, they share underlying structure), optimizing one can initially improve the other; once the shared structure is exhausted, trade-offs dominate again, yielding dominated points.
- **Training unsaturation:** In Fig. 9 (g) and (h), the edge points are mixed together on the top-left corner because iteration 1 for OCR uses much fewer training steps (650) than iteration 0 (1,250); additional training may further improve performance.

Evaluation details:

- **3D Pareto fronts:** For each merge, we evaluate thirteen model weight configurations with different coefficient ratios: three single-reward configurations (the other two coefficients set to zero) and ten mixed configurations. The specific {GenEval: PickScore: OCR} ratios are {1 : 0 : 0}, {0 : 1 : 0}, {0 : 0 : 1}, {0.8 : 0.1 : 0.1}, {0.1 : 0.8 : 0.1}, {0.1 : 0.1 : 0.8}, {0.6 : 0.2 : 0.2}, {0.2 : 0.6 : 0.2}, {0.2 : 0.2 : 0.6}, {0.4 : 0.4 : 0.2}, {0.4 : 0.2 : 0.4}, {0.2 : 0.4 : 0.4}, and {0.3 : 0.3 : 0.3}. Each plotted point is obtained by evaluating one merged model on all three metrics.
- **2D Pareto fronts:** For each merge, we evaluate eleven model weight configurations with different ratios: two single-reward configurations (the other coefficient set to zero) and nine mixed configurations. The specific ratios are {1 : 0}, {0 : 1}, {0.1 : 0.9}, {0.2 : 0.8}, {0.3 : 0.7}, {0.4 : 0.6}, {0.5 : 0.5}, {0.6 : 0.4}, {0.7 : 0.3}, {0.8 : 0.2}, and {0.9 : 0.1}. Each point is obtained by evaluating one merged model on the two metrics.

D.2. Pareto Front Comparison of MORL vs. MapReduce LoRA

To compare naive multi-objective RL with data mixing (MORL-D) against MapReduce LoRA, we train MORL-D under

ten {GenEval:PickScore:OCR} sampling ratios—{1:1:1}, {1:2:3}, {1:3:2}, {2:1:3}, {2:3:1}, {3:1:2}, {3:2:1}, {1:1:4}, {1:4:1}, {4:1:1}—using the same number of training steps as MapReduce LoRA on SD 3.5 M [2]. Fig. 10 compares Pareto fronts for Rewarded Soup [36], MORL-D, and MapReduce LoRA (left: 3D; right: 2D projections). In 3D, MORL-D is confined to a small region across the three rewards. For readability, we also show 2D projections of the 3D front; because MORL-D is an a priori method, we cannot fix one reward to 0 as in Fig. 9, so the right panels are projections rather than true 2D Pareto fronts. Although MORL-D is competitive on GenEval and OCR, conflicting objectives reduce visual quality (PickScore; see Fig. 16), yielding only limited PickScore gains.

Table 5. 3D merging results on Text-to-Image tasks: SD 3.5 M [2] and FLUX.1-dev [20].

Group	Merging Ratios			SD 3.5 M			FLUX.1-dev		
	GenEval	PickScore	OCR	GenEval	PickScore	OCR	GenEval	PickScore	OCR
base model	0	0	0	0.68	21.784	0.601	0.67	22.006	0.573
Merge 1	1	0	0	0.93	21.852	0.658	0.90	22.057	0.692
	0	1	0	0.76	23.359	0.716	0.70	23.566	0.723
	0	0	1	0.68	21.800	0.934	0.68	21.997	0.971
	0.8	0.1	0.1	0.90	21.993	0.704	0.88	22.175	0.756
	0.1	0.8	0.1	0.77	23.090	0.746	0.75	23.408	0.794
	0.1	0.1	0.8	0.70	21.948	0.911	0.71	22.136	0.959
	0.6	0.2	0.2	0.86	22.106	0.743	0.83	22.299	0.802
	0.2	0.6	0.2	0.78	22.731	0.781	0.76	23.046	0.827
	0.2	0.2	0.6	0.76	22.087	0.882	0.73	22.288	0.928
	0.4	0.4	0.2	0.81	22.382	0.758	0.81	22.633	0.813
	0.4	0.2	0.4	0.80	22.098	0.826	0.79	22.294	0.883
	0.2	0.4	0.4	0.77	22.374	0.836	0.76	22.636	0.886
	0.3	0.3	0.3	0.79	22.276	0.805	0.77	22.503	0.868
Merge 2	1	0	0	0.92	22.101	0.802	0.91	22.156	0.844
	0	1	0	0.79	23.205	0.793	0.80	23.515	0.833
	0	0	1	0.74	21.986	0.945	0.71	22.116	0.953
	0.8	0.1	0.1	0.90	22.208	0.831	0.89	22.303	0.883
	0.1	0.8	0.1	0.82	23.004	0.820	0.81	23.337	0.888
	0.1	0.1	0.8	0.76	22.109	0.933	0.75	22.249	0.956
	0.6	0.2	0.2	0.89	22.316	0.839	0.88	22.437	0.913
	0.2	0.6	0.2	0.84	22.778	0.843	0.83	23.037	0.916
	0.2	0.2	0.6	0.81	22.232	0.917	0.80	22.405	0.941
	0.4	0.4	0.2	0.85	22.532	0.850	0.85	22.718	0.918
	0.4	0.2	0.4	0.84	22.290	0.895	0.85	22.429	0.927
	0.2	0.4	0.4	0.83	22.486	0.899	0.81	22.709	0.929
	0.3	0.3	0.3	0.84	22.436	0.871	0.84	22.619	0.926
Merge 3	1	0	0	0.92	22.138	0.854	0.93	22.115	0.894
	0	1	0	0.82	23.243	0.850	0.79	23.902	0.904
	0	0	1	0.78	22.128	0.954	0.77	22.167	0.963
	0.8	0.1	0.1	0.92	22.281	0.890	0.91	22.324	0.928
	0.1	0.8	0.1	0.83	23.080	0.875	0.85	23.683	0.930
	0.1	0.1	0.8	0.81	22.248	0.944	0.80	22.331	0.960
	0.6	0.2	0.2	0.91	22.408	0.900	0.90	22.508	0.936
	0.2	0.6	0.2	0.85	22.869	0.887	0.87	23.285	0.938
	0.2	0.2	0.6	0.84	22.369	0.929	0.85	22.496	0.955
	0.4	0.4	0.2	0.88	22.637	0.904	0.90	22.878	0.934
	0.4	0.2	0.4	0.87	22.393	0.920	0.88	22.515	0.943
	0.2	0.4	0.4	0.85	22.615	0.913	0.86	22.864	0.946
	0.3	0.3	0.3	0.88	22.554	0.908	0.88	22.740	0.941

Table 6. 2D merging results on Text-to-Image tasks, SD 3.5 M [2] and FLUX.1-dev [20], and Text-to-Video task, HunyuanVideo [19].

Group	Merging Ratios		SD 3.5 M				FLUX.1-dev				HunyuanVideo					
	reward A	reward B	^A GenEval	^B PickScore	^A GenEval	^B OCR	^A PickScore	^B OCR	^A GenEval	^B PickScore	^A GenEval	^B OCR	^A PickScore	^B OCR	^A VQ	^B MQ
base model	0	0	0.68	21.784	0.68	0.601	21.784	0.601	0.67	22.006	0.67	0.573	22.006	0.573	3.25	0.95
Merge 1	0	1	0.76	23.359	0.68	0.934	21.800	0.934	0.70	23.566	0.68	0.971	21.997	0.971	3.80	1.66
	0.1	0.9	0.77	23.233	0.71	0.923	21.926	0.925	0.74	23.525	0.68	0.966	22.122	0.972	3.89	1.62
	0.2	0.8	0.79	23.084	0.73	0.904	22.062	0.909	0.77	23.403	0.71	0.962	22.260	0.968	3.95	1.57
	0.3	0.7	0.83	22.923	0.75	0.891	22.207	0.903	0.79	23.220	0.72	0.946	22.436	0.946	4.01	1.52
	0.4	0.6	0.83	22.736	0.78	0.864	22.358	0.878	0.80	23.024	0.75	0.929	22.627	0.930	4.06	1.48
	0.5	0.5	0.85	22.549	0.82	0.838	22.534	0.861	0.83	22.825	0.79	0.899	22.828	0.916	4.13	1.43
	0.6	0.4	0.88	22.379	0.86	0.811	22.715	0.848	0.85	22.629	0.81	0.862	23.032	0.891	4.18	1.38
	0.7	0.3	0.90	22.232	0.86	0.766	22.902	0.803	0.86	22.446	0.83	0.831	23.242	0.857	4.23	1.34
	0.8	0.2	0.90	22.093	0.89	0.734	23.085	0.782	0.87	22.297	0.87	0.787	23.410	0.823	4.29	1.30
	0.9	0.1	0.92	21.966	0.91	0.706	23.237	0.754	0.88	22.169	0.89	0.742	23.530	0.785	4.33	1.25
1	0	0.93	21.852	0.93	0.658	23.359	0.716	0.90	22.057	0.90	0.692	23.566	0.723	4.37	1.20	
Merge 2	0	1	0.79	23.205	0.74	0.945	21.986	0.945	0.80	23.515	0.71	0.953	22.116	0.953	4.18	1.84
	0.1	0.9	0.81	23.125	0.76	0.945	22.090	0.943	0.82	23.447	0.74	0.945	22.241	0.945	4.25	1.80
	0.2	0.8	0.82	23.039	0.77	0.935	22.178	0.931	0.83	23.332	0.75	0.952	22.377	0.948	4.32	1.77
	0.3	0.7	0.84	22.930	0.80	0.925	22.307	0.924	0.85	23.195	0.80	0.950	22.524	0.953	4.40	1.73
	0.4	0.6	0.86	22.817	0.81	0.915	22.421	0.917	0.86	23.040	0.82	0.939	22.696	0.947	4.46	1.70
	0.5	0.5	0.87	22.699	0.84	0.897	22.557	0.902	0.88	22.867	0.83	0.931	22.856	0.934	4.52	1.67
	0.6	0.4	0.90	22.569	0.86	0.897	22.706	0.884	0.88	22.713	0.87	0.933	23.017	0.927	4.56	1.63
	0.7	0.3	0.90	22.438	0.88	0.871	22.849	0.872	0.90	22.557	0.89	0.918	23.189	0.914	4.60	1.60
	0.8	0.2	0.90	22.318	0.90	0.856	22.977	0.847	0.89	22.418	0.89	0.907	23.339	0.907	4.63	1.56
	0.9	0.1	0.91	22.208	0.91	0.826	23.100	0.823	0.90	22.282	0.90	0.872	23.450	0.879	4.66	1.53
1	0	0.92	22.101	0.92	0.802	23.205	0.793	0.91	22.156	0.91	0.844	23.515	0.833	4.70	1.50	
Merge 3	0	1	0.82	23.243	0.78	0.954	22.128	0.954	0.79	23.902	0.77	0.963	22.167	0.963	4.59	1.84
	0.1	0.9	0.83	23.179	0.79	0.949	22.238	0.951	0.83	23.844	0.78	0.962	22.316	0.951	4.64	1.82
	0.2	0.8	0.84	23.097	0.82	0.947	22.338	0.940	0.87	23.693	0.82	0.960	22.467	0.952	4.67	1.82
	0.3	0.7	0.87	23.003	0.83	0.936	22.454	0.931	0.90	23.504	0.84	0.962	22.642	0.956	4.71	1.82
	0.4	0.6	0.89	22.892	0.86	0.931	22.578	0.939	0.90	23.299	0.86	0.958	22.834	0.955	4.77	1.81
	0.5	0.5	0.91	22.772	0.88	0.920	22.699	0.924	0.93	23.091	0.87	0.950	23.046	0.949	4.81	1.81
	0.6	0.4	0.90	22.640	0.90	0.914	22.842	0.915	0.92	22.872	0.90	0.946	23.263	0.948	4.85	1.79
	0.7	0.3	0.90	22.504	0.90	0.902	22.955	0.908	0.93	22.680	0.90	0.943	23.467	0.939	4.91	1.79
	0.8	0.2	0.92	22.375	0.91	0.896	23.055	0.891	0.93	22.485	0.91	0.936	23.666	0.937	4.95	1.77
	0.9	0.1	0.91	22.261	0.92	0.890	23.164	0.868	0.92	22.301	0.91	0.922	23.838	0.919	4.99	1.77
1	0	0.92	22.138	0.92	0.854	23.243	0.850	0.93	22.115	0.93	0.894	23.902	0.904	5.03	1.75	

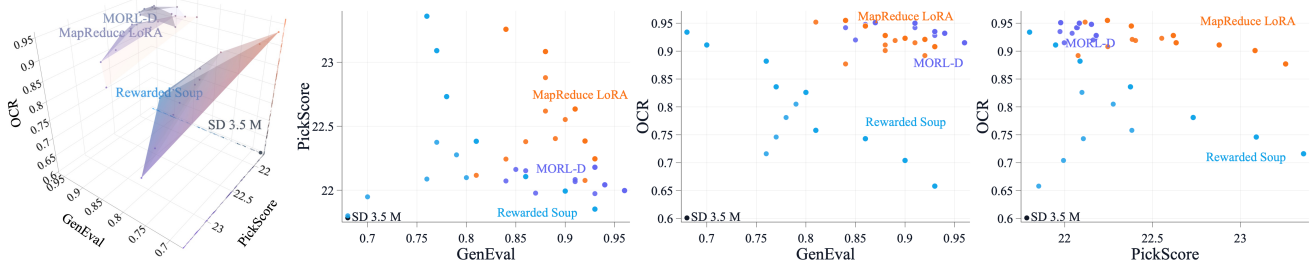


Figure 10. Merging performance comparison across Rewarded Soup [36], MORL-D, and MapReduce LoRA. Left: 3D Pareto-front comparison. Right: 2D projections of the 3D Pareto front (for readability), which are not 2D Pareto fronts. Unlike Fig. 9, these are projections rather than a 2D merge with the third reward fixed to 0. MORL-D performance is confined to a small region across the three rewards and yields only limited improvement on PickScore.

D.3. Scalability of Reward Numbers

We extend MapReduce LoRA to 5 rewards by adding VQAScore [24] and MPS [47] on SD 3.5 M [2]. Fig. 11 shows that MapReduce LoRA improves all 5 rewards (+22% GenEval, +3% PickScore, +44% OCR, +6% VQAScore, +7% MPS), consistently outperforming one-shot Rewarded Soup (the starting point of $k = 1$). Scaling to more rewards does not introduce diminishing returns: performance on overlapping rewards (GenEval, PickScore, OCR) remains improved compared to 3-reward training (Fig. 6, $k=4$). However, achieving similar levels requires 1.66 \times more steps, reflecting increased optimization complexity. Beyond the increased optimization complexity for existing rewards, adding rewards incurs a linear per-reward training cost; however, the parallel Map phase helps mitigate the resulting wall-clock growth given sufficient GPUs.

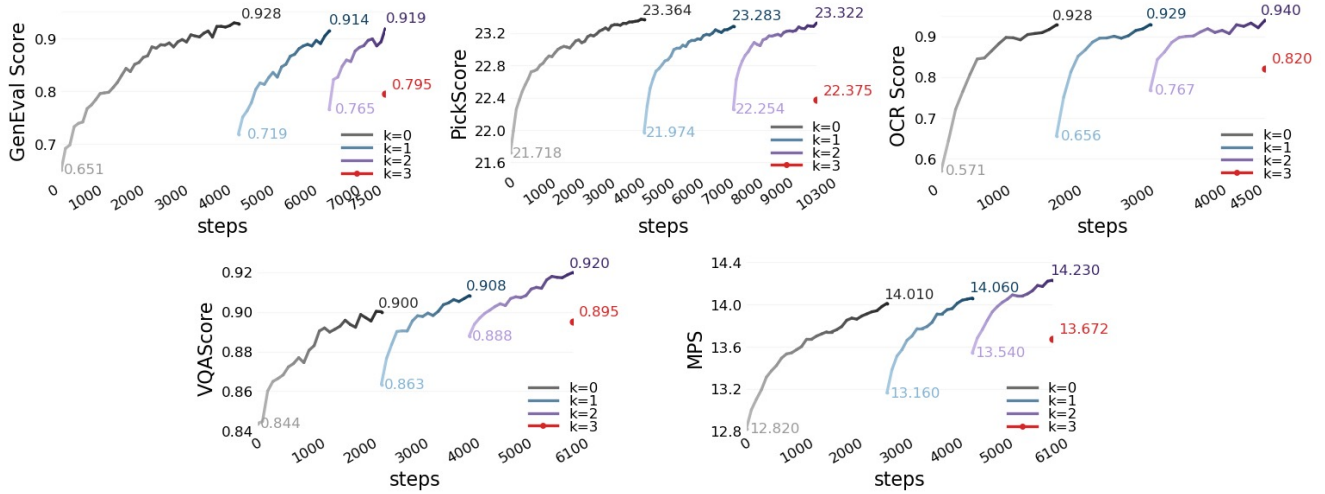


Figure 11. MapReduce LoRA across 5 rewards with 3 merges.

E. More Qualitative Results

E.1. Text-to-Image qualitative results

Figs 12, 13 and 14 demonstrate the visual comparison of two rewards with different merging ratios. Figs 15 and 16 demonstrate the visual comparison of all methods, including Flow-GRPO [26] tuned on GenEval [14], PickScore [18], OCR [8], Rewarded Soup [36], MORL-D, MORL-DR and MapReduce LoRA. PickScore and OCR guidance cause strong reward overfitting: the former drives the model toward a narrow, high-scoring aesthetic style, while the latter encourages increasingly large and prominent text regardless of overall visual harmony or contextual appropriateness. Our proposed MapReduce LoRA mitigates these issues by iteratively merging per-reward experts, enabling the model to discover a more balanced (and often near-optimal) preference that harmonizes aesthetic fidelity with text readability.



Figure 12. Visual comparison across different merging ratios between PickScore and GenEval.

PickScore ← $\{1:0\}$ $\{0.9:0.1\}$ $\{0.8:0.2\}$ $\{0.7:0.3\}$ $\{0.6:0.4\}$ $\{0.5:0.5\}$ $\{0.4:0.6\}$ $\{0.3:0.7\}$ $\{0.2:0.8\}$ $\{0.1:0.9\}$ → OCR



A high-fashion runway with a sleek, modern backdrop displaying "Spring Collection 2024". Models walk confidently on the catwalk, showcasing vibrant, floral prints and pastel tones, under soft, ambient lighting that enhances the fresh, spring vibe.



A realistic photograph of a fast food drive-thru menu board at dusk, featuring a bold and colorful advertisement that reads "Try Our New Burger" with an appetizing image of the burger below, set against the backdrop of a busy suburban street.



A high-altitude mountain summit with a wooden signpost clearly marked "Elevation 8000 Feet", surrounded by rocky terrain and a backdrop of distant, snow-capped peaks under a clear blue sky.



A weathered pirate ship flag, tattered and fluttering in the sea breeze, is intricately embroidered with the bold words "Sea Wolf Crew" in deep navy thread, against a backdrop of stormy skies and turbulent waves.



An astronaut in space, the helmet visor reflecting a floating "Low Oxygen Warning" sign, surrounded by the vast, star-filled darkness, with Earth faintly visible in the distance.



A bustling deli with vintage decor, the counter lined with gleaming metal and glass. A retro ticket machine in the corner, lights blinking, prints out a paper slip that reads "Now Serving 42", amid the hum of conversation and the scent of fresh bread.



A UFO hovers in the night sky, its underside glowing with a soft, otherworldly light. Beneath it, a beam of light illuminates a peaceful landscape. The words "We Come in Peace" are clearly visible on its surface, radiating a sense of calm and hope.



A vibrant skatepark with dynamic graffiti tagging that reads "Skate Or Die Trying" across a worn, concrete wall, surrounded by skaters performing tricks and an urban backdrop.



A vintage suitcase adorned with a "World Traveler Adventures" sticker, placed on a rustic wooden table. Sunlight filters through a nearby window, casting warm, golden hues on the suitcase and highlighting the sticker's faded, nostalgic colors.

Figure 13. Visual comparison across different merging ratios between PickScore and OCR.



Figure 14. Visual comparison across different merging ratios between GenEval and OCR.

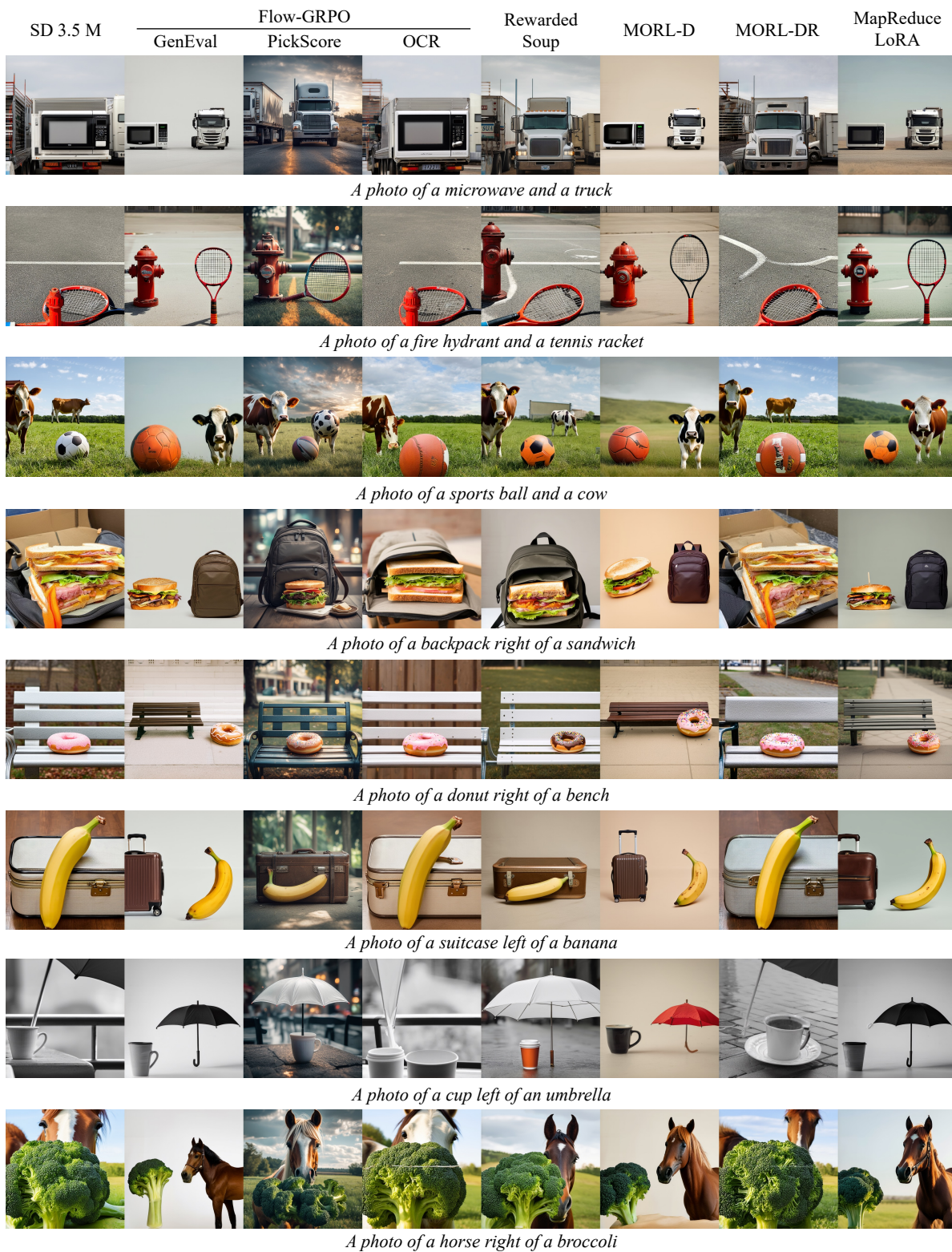


Figure 15. Visual comparison across all methods.



A realistic cockpit interior with a digital screen displaying "Prepare for Landing" in bold text, illuminated by soft blue backlighting, with the pilot's hand resting on the control yoke.



A bustling city street at night with a movie theater marquee prominently displaying "Now Showing Action 5". Crowds of people in casual attire are entering the theater, while neon lights and billboards light up the background, creating a vibrant urban atmosphere.



A bustling stadium at dusk, the scoreboard prominently displays "Home Team Wins" in vibrant, illuminated letters, surrounded by cheering fans in team colors, with the victorious team's players celebrating on the field.



A beekeeper stands beside a wooden hive box, carefully labeled "Buzz Central Handle With Care", surrounded by a bustling field of wildflowers, with bees fluttering around the hive and the keeper wearing traditional protective gear.



A realistic photograph of a gas station with a large, red price sign prominently displaying "Fuel Prices Rising" against a cloudy sky, cars filling up in the background.



A detailed close-up of a magic carpet with intricate embroidery, prominently featuring the text "No Shoes Fly Casual" woven in shimmering threads, set against a backdrop of a serene, cloudy sky.



A movie poster titled "Invasion of the Robots" featuring towering robots destroying cityscapes, with skyscrapers collapsing and fiery explosions lighting up the night sky, emphasizing the chaos and scale of the robotic invasion.

Figure 16. Visual comparison across all methods on text rendering quality.

E.2. Text-to-Video qualitative results

Fig. 17 demonstrates the visual comparison of HunyuanVideo [19], Rewarded Soup [36] and our proposed MapReduce LoRA. Also, Figs. 18 and 19 demonstrate the visual performance of merging progress that advances the visual quality, motion quality, and prompt alignment.

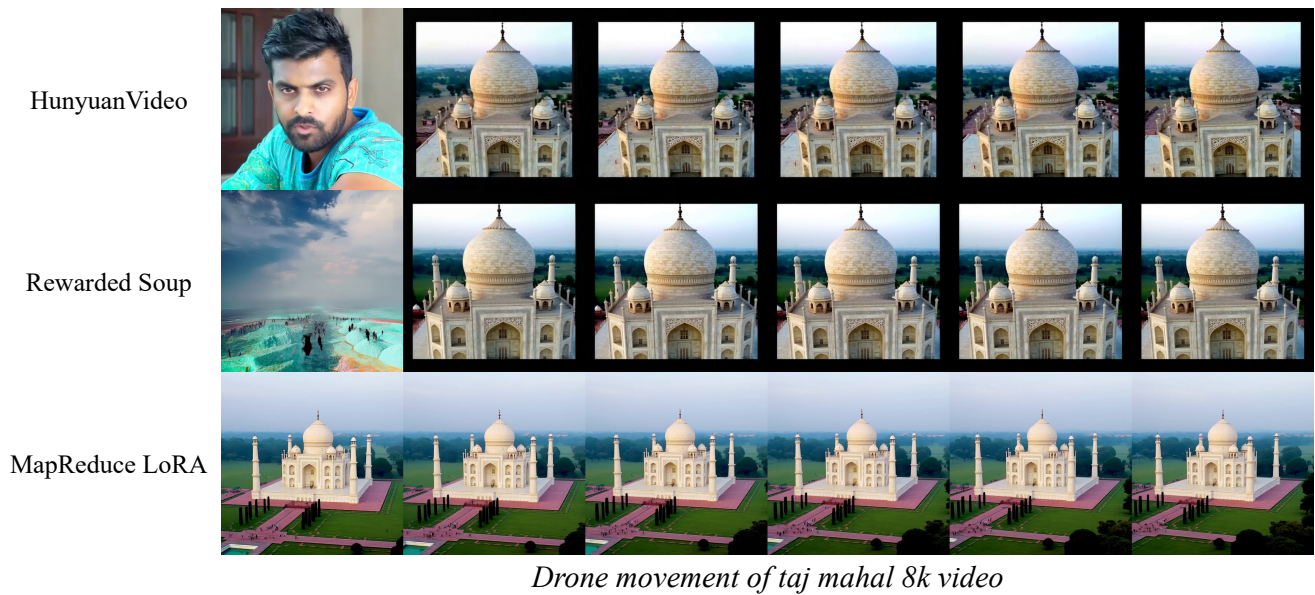
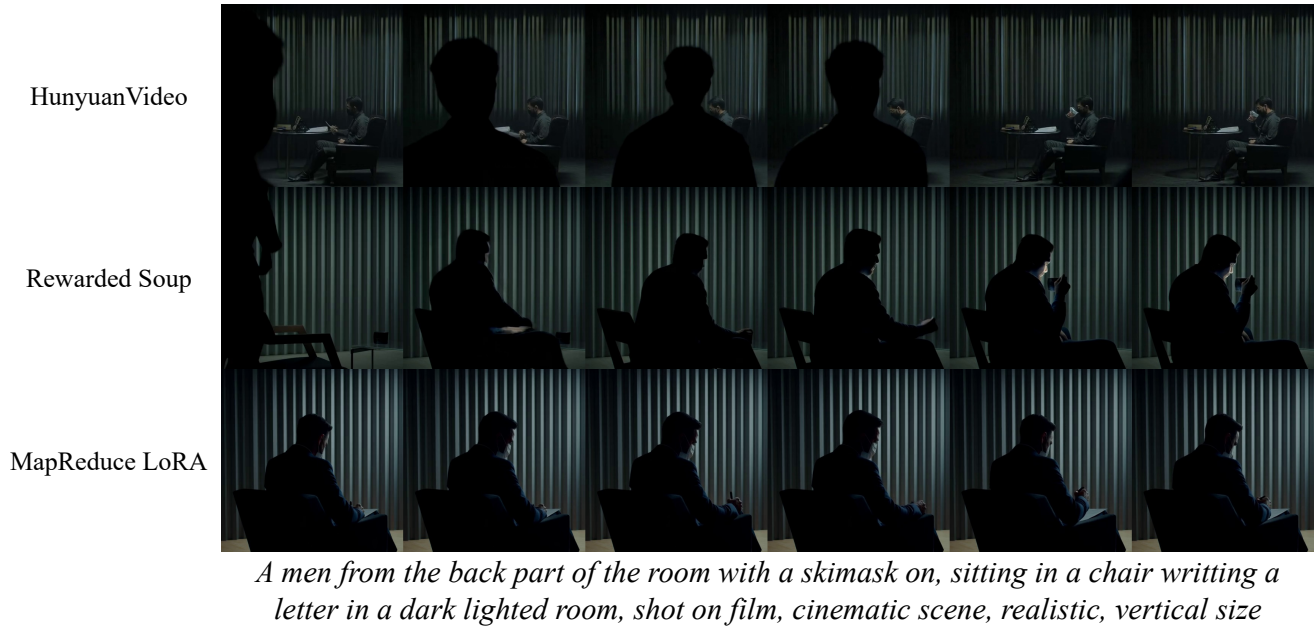


Figure 17. **Visual comparison of HunyuanVideo [19], Rewarded Soup [36], and MapReduce LoRA (Ours).** In the upper case, MapReduce LoRA more faithfully renders the intended motion and writing action described in the prompt. In the lower case, MapReduce LoRA better adheres to the specified drone-movement control, producing a trajectory that aligns with the prompt.



Deadpool walking around in an cyber city



An interesting visual for an industrial techno party

Figure 18. **Visual performance across two cases under different MapReduce LoRA merging iterations.** In the upper case, the HunyuanVideo result fails to depict the walking motion, while increasing the merging iterations progressively restores natural walking dynamics and improves the background building quality. In the lower case, the initial generation shows limited visual fidelity, whereas successive merging iterations consistently enhance the overall clarity and scene quality.

HunyuanVideo



MapReduce LoRA (merge 1)



MapReduce LoRA (merge 2)



MapReduce LoRA (merge 3)



Korean pregnant woman holding baby while selfie with iphone

HunyuanVideo



MapReduce LoRA (merge 1)



MapReduce LoRA (merge 2)



MapReduce LoRA (merge 3)



Two people sitting on the beach drinking, cozy images, the sound of waves, seagulls

Figure 19. **Visual performance across two cases under different MapReduce LoRA merging iterations.** In the upper case, the HunyuanVideo result shows limited visual clarity—partly due to suboptimal motion quality—while increasing merging iterations progressively refine facial and background details, improve pose naturalness, and enhance overall realism. In the lower case, the initial generation offers limited scene clarity—the drinking containers are barely visible—whereas additional merging iterations clearly render these objects and deliver sharper, more coherent visuals.

F. Limitations and Future Works

This paper presents MapReduce LoRA, a simple, scalable recipe for systematically pushing the multi-preference Pareto front and enabling practical post-training customization. We note several scope considerations and opportunities for further study:

- **Scaling to more preferences:** In Text-to-Image, we validate on five targeted preferences; extending to larger numbers of preferences is a promising scaling direction.
- **Merging policies and schedules:** We default to uniform averaging and compare a few merge frequencies under fixed training steps; exploring adaptive/learned policies and schedules may yield further gains.
- **Architecture-agnostic Reward-aware Token Embedding (RaTE):** RaTE is lightweight and effective on Stable Diffusion series models, which contain explicit cross-attention between text and image information, but is less reliable for joint sequence models, *i.e.*, FLUX. Exploring model-agnostic designs is a practical direction.

We leave these promising directions for future work.